

# Major Changes in 2021 World Health Organization Classification of Central Nervous System Tumors

Ryo Kurokawa, MD, PhD

Mariko Kurokawa, MD

Akira Baba, MD, PhD

Yoshiaki Ota, MD

Emile Pinarbasi, MD, PhD

Sandra Camelo-Piragua, MD

Aristides A. Capizzano, MD

Eric Liao, MD

Ashok Srinivasan, MD

Toshio Moritani, MD, PhD

**Abbreviations:** cIMPACT-NOW = Consortium to Inform Molecular and Practical Approaches to CNS Tumor Taxonomy; CNS = central nervous system; FET =  $O$ - $(2-[^{18}\text{F}]\text{fluoroethyl})$ - $\text{l}$ -tyrosine; FLAIR = fluid-attenuated inversion recovery; H-E = hematoxylin-eosin; HGAP = high-grade astrocytoma with piloid features; MAPK = mitogen-activated protein kinase; MVNT = multinodular and vacuolating neuronal tumor; PLNTY = polymorphous low-grade neuroepithelial tumor of the young; WHO = World Health Organization; WHO CNS5 = *WHO Classification of Tumors of the Central Nervous System* fifth edition

**RadioGraphics** 2022; 42:1474–1493

<https://doi.org/10.1148/rg.210236>

**Content Codes:** **MR** **NR**

From the Division of Neuroradiology, Department of Radiology (R.K., M.K., A.B., Y.O., A.A.C., E.L., A.S., T.M.) and Department of Pathology (E.P., S.C.P.), Michigan Medicine, University of Michigan, 1500 E Medical Center Dr, UH B2, Ann Arbor, MI 48109; and Department of Radiology, Graduate School of Medicine, The University of Tokyo, Tokyo, Japan (R.K., M.K.). Presented as an education exhibit at the 2021 RSNA Annual Meeting. Received January 4, 2022; revision requested March 16 and received March 21; accepted March 25. For this journal-based SA-CME activity, the author E.L. has provided disclosures (see end of article); all other authors, the editor, and the reviewers have disclosed no relevant relationships. **Address correspondence to** R.K. (e-mail: [kuro63@gmail.com](mailto:kuro63@gmail.com)).

©RSNA, 2022

## SA-CME LEARNING OBJECTIVES

After completing this journal-based SA-CME activity, participants will be able to:

- Describe the major changes in WHO CNS5.
- Become familiar with the genetic and molecular mechanisms of tumorigenesis of newly recognized tumor types.
- List the imaging features of various newly recognized tumor types.

*See [rsna.org/learning-center-rg](http://rsna.org/learning-center-rg).*

The World Health Organization (WHO) published the fifth edition of the *WHO Classification of Tumors of the Central Nervous System* (WHO CNS5) in 2021, as an update of the WHO central nervous system (CNS) classification system published in 2016. WHO CNS5 was drafted on the basis of recommendations from the Consortium to Inform Molecular and Practical Approaches to CNS Tumor Taxonomy (cIMPACT-NOW) and expounds the classification scheme of the previous edition, which emphasized the importance of genetic and molecular changes in the characteristics of CNS tumors. Multiple newly recognized tumor types, including those for which there is limited knowledge regarding neuroimaging features, are detailed in WHO CNS5. The authors describe the major changes introduced in WHO CNS5, including revisions to tumor nomenclature. For example, WHO grade IV tumors in the fourth edition are equivalent to CNS WHO grade 4 tumors in the fifth edition, and diffuse midline glioma, *H3 K27M*-mutant, is equivalent to midline glioma, *H3 K27*-altered. With regard to tumor typing, isocitrate dehydrogenase (*IDH*)-mutant glioblastoma has been modified to *IDH*-mutant astrocytoma. In tumor grading, *IDH*-mutant astrocytomas are now graded according to the presence or absence of homozygous *CDKN2A/B* deletion. Moreover, the molecular mechanisms of tumorigenesis, as well as the clinical characteristics and imaging features of the tumor types newly recognized in WHO CNS5, are summarized. Given that WHO CNS5 has become the foundation for daily practice, radiologists need to be familiar with this new edition of the WHO CNS tumor classification system.

*Online supplemental material and the slide presentation from the RSNA Annual Meeting are available for this article.*

©RSNA, 2022 • [radiographics.rsna.org](http://radiographics.rsna.org)

## Introduction

The World Health Organization (WHO) published the fifth edition of the *WHO Classification of Tumors of the Central Nervous System* (WHO CNS5) in 2021, as an update of the fourth edition of this classification system, which was published in 2016 (1,2). This latest classification system was implemented on the basis of recommendations from the Consortium to Inform Molecular and Practical Approaches to CNS Tumor Taxonomy (cIMPACT-NOW), a task force that has summarized a number of statements regarding tumor nomenclature, typing, and grading in a series of reports (3–9).

In this article, to facilitate understanding of WHO CNS5, we (a) provide a brief history of the WHO classification of central nervous system (CNS) tumors and a summary of cIMPACT-NOW proposal updates; (b) review the molecular and genetic profiles in WHO CNS5, including *IDH*-mutant and *IDH*-wildtype grading of gliomas; and (c) describe the molecular, clinical, and imaging features of the newly recognized CNS tumor types.

## TEACHING POINTS

- In the WHO CNS tumor classification update, published in 2016, a diagnostic framework based on the molecular and genetic features of CNS tumors was adopted, and a layered reporting system consisting of integrated diagnosis, histologic diagnosis, WHO grading, and molecular information was incorporated.
- *IDH*-mutant astrocytomas are classified as CNS WHO grade 2, 3, or 4 in WHO CNS5, depending on the presence or absence of homozygous deletions of *CDKN2A/B*, which are a negative prognostic factor.
- For adult-type *IDH*-wildtype diffuse astrocytic gliomas, the diagnosis of glioblastoma, *IDH*-wildtype, should be determined on the basis of the presence of necrosis and/or florid microvascular proliferation (the conventional criterion), and/or at least one of the following three criteria: concurrent gain of the whole chromosome 7 and loss of the whole chromosome 10 (+7/-10), *TERT* promoter mutations, and *EGFR* amplification.
- In WHO CNS5, owing to their distinct clinical appearance, *IDH*-wildtype diffuse gliomas that mainly affect pediatric patients (ie, pediatric diffuse gliomas) are classified separately from *IDH*-wildtype diffuse gliomas that occur in adults. Pediatric diffuse gliomas are classified into low- and high-grade groups.
- Three newly recognized provisional tumor types were introduced in WHO CNS5: *diffuse glioneuronal tumors with oligodendrogloma-like features and nuclear clusters; cribriform neuroepithelial tumors; and intracranial mesenchymal tumors, FET-CREB fusion-positive*. These provisional tumors currently await comprehensive published characterization but will likely become fully recognized tumor types in a future classification iteration.

## History of WHO Classification and Proposals of cIMPACT-NOW Updates

The first edition of the WHO classification of CNS tumors was published in 1979 to promote international comparative studies of CNS tumors, establish histologic criteria, and standardize tumor nomenclature (10). In the first edition, the grading system (grades I–IV) reflecting clinicohistologic features was declared to be applicable to the field of CNS tumors, and the concept of anaplasia was introduced. In the second edition that followed in 1993, technical advances were incorporated and immunohistochemical features were integrated (11,12). In the third edition, published in 2000, the results of the evolving molecular biologic studies of CNS tumors (13) were incorporated, and a system of shared writing by working groups, consisting of several authors for each chapter, was introduced. In the fourth edition, published in 2007, tumor groups were classified, by independency, as tumors with clear independence (entity), a group of tumors with weak independence (variant), and a group of tumors with a tumor morphology of unknown independence (pattern). However, the terms *entity* and *variant* were replaced by *type* and *subtype*, respectively, in the latest edition (2,14).

In the WHO CNS tumor classification update, published in 2016, a diagnostic framework based on the molecular and genetic features of CNS tumors (1) was adopted, and a layered reporting system consisting of integrated diagnosis, histologic diagnosis, WHO grading, and molecular information was incorporated. In addition, a revision of the diagnostic criteria for adult diffuse gliomas based on the presence or absence of isocitrate dehydrogenase (*IDH*) gene mutation and the presence or absence of 1p/19q codeletion was appended in the 2016 edition (1).

After publication of the 2016 edition of the WHO CNS tumor classification system, cIMPACT-NOW was established to improve the diagnosis and classification of CNS tumors. The major changes made in WHO CNS5, in response to the cIMPACT-NOW proposals, are summarized in Table E1. In cIMPACT-NOW update 1, the terms *not otherwise specified* and *not elsewhere classified* are defined and used to classify some tumor groups (3,15). Update 2 clarified the diagnosis of diffuse midline glioma, *H3 K27M*-mutant, and *IDH*-mutant diffuse astrocytoma or anaplastic astrocytoma (4). In update 3, a proposal to recognize histologically lower-grade *IDH*-wildtype diffuse astrocytic gliomas as glioblastoma, depending on the following molecular features, was introduced: concurrent gain of the whole chromosome 7 and loss of the whole chromosome 10 (+7/-10); *TERT* promoter mutations; and *EGFR* amplification (5).

Update 4 emphasized the importance of further characterizing the genetic features of *IDH*- and *H3*-wildtype diffuse pediatric gliomas (6). In update 5, it was recommended that the grading of *IDH*-mutant astrocytomas be based on *CDKN2A/B* homozygous deletion status (7). Update 6 included recommendations regarding a number of new tumor types and diagnostic principles (8). In update 7, the classification of ependymomas was refined by using molecular features (9).

## Emphasis on Genetic and Molecular Profiles in WHO CNS5

The classification scheme in the 2016 edition of the WHO CNS tumor classification system, which emphasized the mechanisms through which molecular changes affect the characteristics of CNS tumors, is expounded in WHO CNS5. The reason for this emphasis on molecular genetic diagnosis is the superiority of this approach in terms of tumor classification and correlation with prognosis. The limitations of morphologic classification were acknowledged before the 2016 edition, as demonstrated by the lack of differentiation among molecular findings (ie, *IDH1R132H*,

### Revised CNS Tumor Nomenclature in WHO CNS5

Tumor Name in 2016 WHO Classification	Revised Term(s) in WHO CNS5
Diffuse astrocytoma, <i>IDH</i> -mutant	Astrocytoma, <i>IDH</i> -mutant; CNS WHO grade 2
Anaplastic astrocytoma, <i>IDH</i> -mutant	Astrocytoma, <i>IDH</i> -mutant; CNS WHO grade 3
Glioblastoma, <i>IDH</i> -mutant	Astrocytoma, <i>IDH</i> -mutant; CNS WHO grade 4
Diffuse midline glioma, <i>H3 K27M</i> -mutant	Diffuse midline glioma, <i>H3 K27</i> -altered
Astroblastoma	Astroblastoma, <i>MN1</i> -altered
Ependymoma, <i>RELA</i> fusion-positive	Supratentorial ependymoma, <i>ZFTA</i> fusion-positive
Chordoid glioma of the third ventricle	Chordoid glioma
Embryonal tumor with multilayered rosettes, <i>C19MC</i> -altered	Embryonal tumor with multilayered rosettes
Melanotic schwannoma	Malignant melanotic nerve sheath tumor
Solitary fibrous tumor and hemangiopericytoma	Solitary fibrous tumor
Pituitary adenoma	Pituitary adenoma and PitNET (PitNET added) Mesenchymal chondrosarcoma (formerly recognized as a subtype) Adamantinomatous craniopharyngioma (formerly recognized as a subtype) Papillary craniopharyngioma (formerly recognized as a subtype) Pituicytoma, granular cell tumor of the sellar region, and spindle cell oncocytoma (grouped)

Source.—Adapted and reprinted, with permission, from reference 2.

Note.—PitNET = pituitary neuroendocrine tumor.

*TP53*, *ATRX*, and 1p/19q codeletion) in the morphologic astrocytic and oligodendroglial components of oligoastrocytoma, which was previously considered a mixed glioma (16).

Another factor is that morphology-based diagnosis can be more subjective, with high interrater variability among pathologists (17), as opposed to more objective diagnosis based on the expression of specific molecules or genetic changes. Furthermore, the increased prognostic performance of molecular-genetic diagnosis, as exemplified by the better prognosis associated with *IDH*-mutant gliomas compared with the prognosis associated with *IDH*-wildtype gliomas, regardless of the histologic grade (18), was one of the most important factors behind the molecular classification in the WHO CNS5 and 2016 WHO systems. In WHO CNS5, a number of newly recognized tumor types were introduced, and the nomenclature for some tumors was revised on the basis of recent developments in molecular-genetic diagnosis since the 2016 WHO classification update (Table, Table E2) (2).

### Molecular Grading of *IDH*-Mutant and *IDH*-Wildtype Adult Gliomas

A subset of the molecular findings in WHO CNS5 involve the grading of *IDH*-mutant and *IDH*-wildtype adult gliomas (Fig 1) (2,4,5,7,8,19–21). *IDH*-mutant astrocytomas are

classified as CNS WHO grade 2, 3, or 4 in WHO CNS5, depending on the presence or absence of homozygous deletions of *CDKN2A/B* (2,7), which are a negative prognostic factor (Table E1). This is because the homozygous deletion of *CDKN2A/B* causes an uncontrolled transition from the G1 phase to the S phase, resulting in higher tumor cell proliferation (Figs 2, 3) (12). For adult-type *IDH*-wildtype diffuse astrocytic gliomas, the diagnosis of glioblastoma, *IDH*-wildtype, should be determined on the basis of the presence of necrosis and/or florid microvascular proliferation (the conventional criterion), and/or at least one of the following three criteria: concurrent gain of the whole chromosome 7 and loss of the whole chromosome 10 (+7/-10), *TERT* promoter mutations, and *EGFR* amplification (Fig 4, Table E1) (2,5). With this revision, glioblastoma can now be diagnosed without histopathologic evidence of necrosis or florid microvascular proliferation, as long as any of the three above-mentioned molecular criteria are met (leading to a diagnosis of molecular glioblastoma). This revision is based on the finding that patients with histologic *IDH*-wildtype diffuse astrocytic glioma who have at least one of the aforementioned molecular features have statistically significantly shorter survival times and similarly unfavorable outcomes compared with patients who have *IDH*-wildtype glioblastoma (5).

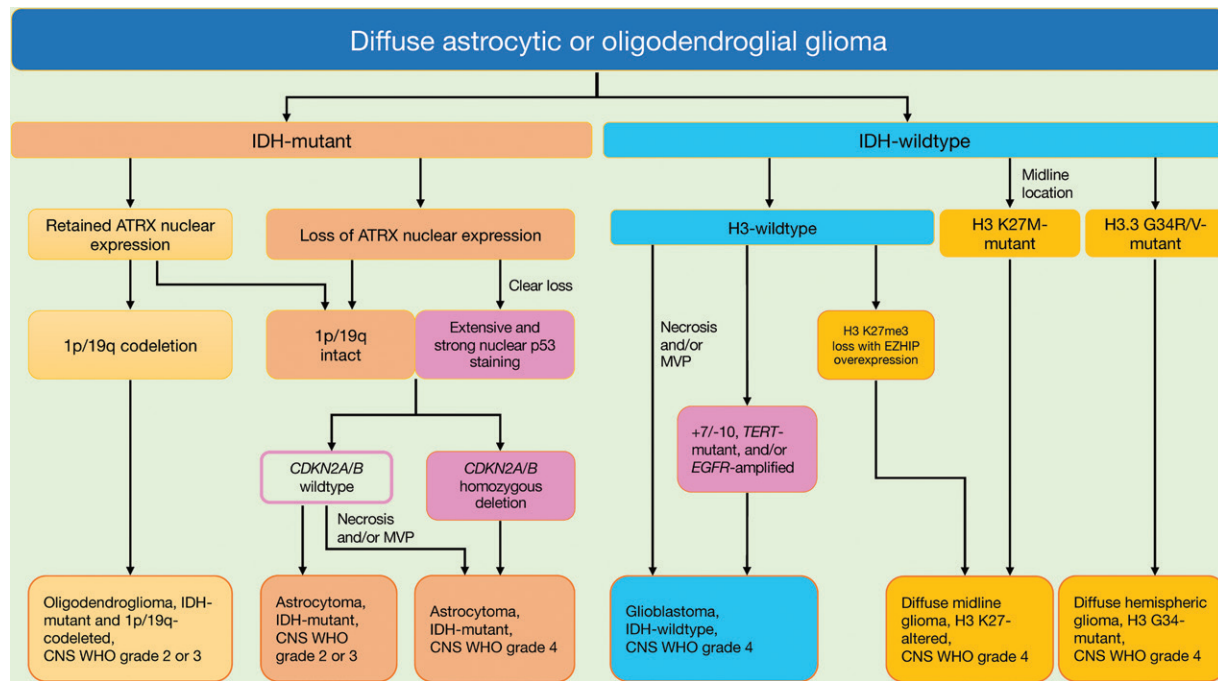


**Figure 1.** Diagnostic flowchart of adult diffuse astrocytic or oligodendroglial glioma. Diffuse gliomas are initially classified as *IDH* mutant or *IDH* wildtype according to the presence or absence of *IDH1* or *IDH2* mutations. *IDH*-mutant gliomas are classified as oligodendroglomas, which show both retained *ATRX* nuclear expression and 1p/19q codeletion, or astrocytomas, which show neither of these findings. *IDH*-mutant astrocytomas are classified as CNS WHO grade 4 tumors if they have necrosis, microvascular proliferation (MVP), or *CDKN2A/B* homozygous deletion (7). *IDH*-wildtype gliomas are classified as diffuse hemispheric glioma, *H3* *G34*-mutant, if they harbor *H3.3 G34R/V* mutation (8,19,20). *IDH*-wildtype gliomas localizing in midline locations (eg, brainstem, thalamus, spinal cord) with *H3* *K27M*-mutant or *H3* *K27me3* loss with *EZH2* overexpression are classified as diffuse midline glioma, *H3* *K27*-altered (4,21). *IDH*-wildtype *H3*-wildtype gliomas without *H3* *K27me3* loss are classified as glioblastoma, *IDH*-wildtype, if they have necrosis, microvascular proliferation, concurrent gain of the whole chromosome 7 and loss of the whole chromosome 10 (+7/-10), *TERT* promoter mutation, and/or *EGFR* amplification (5).

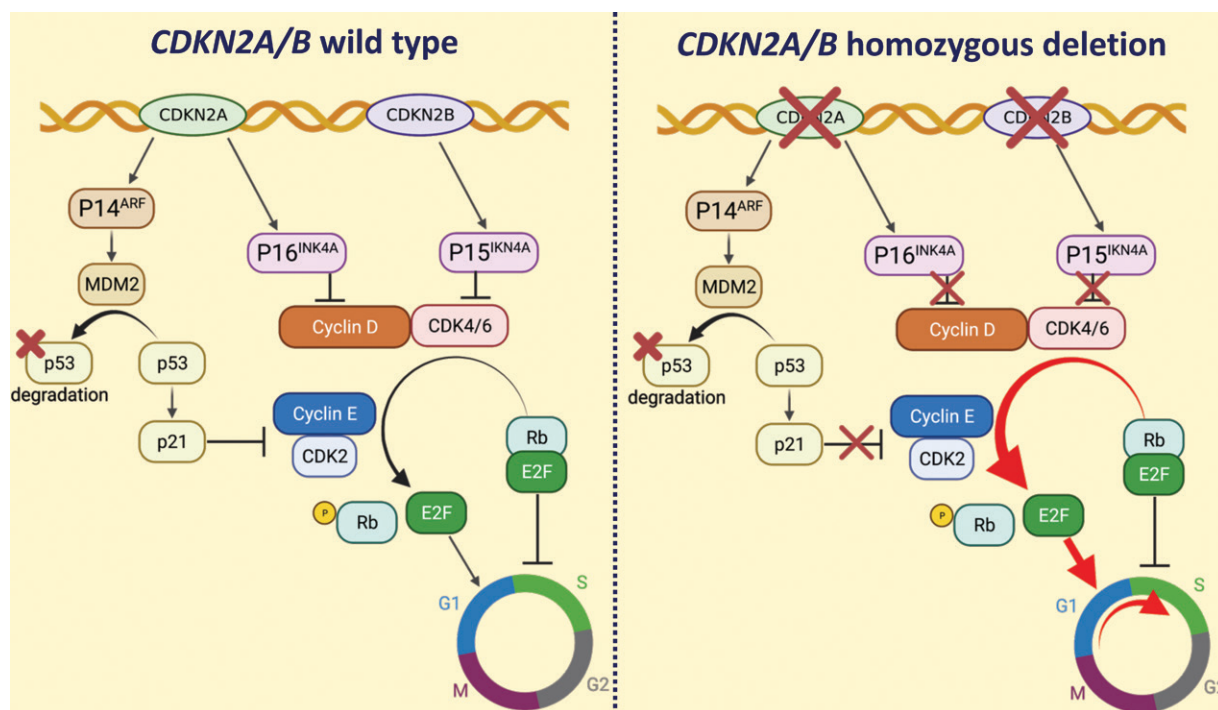


**Figure 2.** Diagrams provide visual depictions of the mechanisms through which homozygous deletions of *CDKN2A/B* act as negative prognostic factors. Left: In *CDKN2A/B* wildtype tumors, the cell cycle is regulated via the modulation of cyclins and cyclin-dependent kinases. Right: Given the homozygous deletion of *CDKN2A/B*, this modulation is suppressed, resulting in an uncontrolled transition from the G1 phase to the S phase and leading to higher cell proliferation (12).

**Figure 3.** *IDH*-mutant CNS WHO grade 4 astrocytoma in a 66-year-old woman who had experienced multiple episodes of right-sided arm noncoordination. (A) Fluid-attenuated inversion-recovery (FLAIR) MR image shows a hyperintense tumor (arrowhead) in the left frontal lobe. (B) On a contrast-enhanced T1-weighted MR image, the tumor (arrowhead) shows patchy enhancement. Although no evidence of necrosis or microvascular proliferation was observed histologically, the tumor was graded as CNS WHO grade 4, given the homozygous deletion of *CDKN2A/B*.

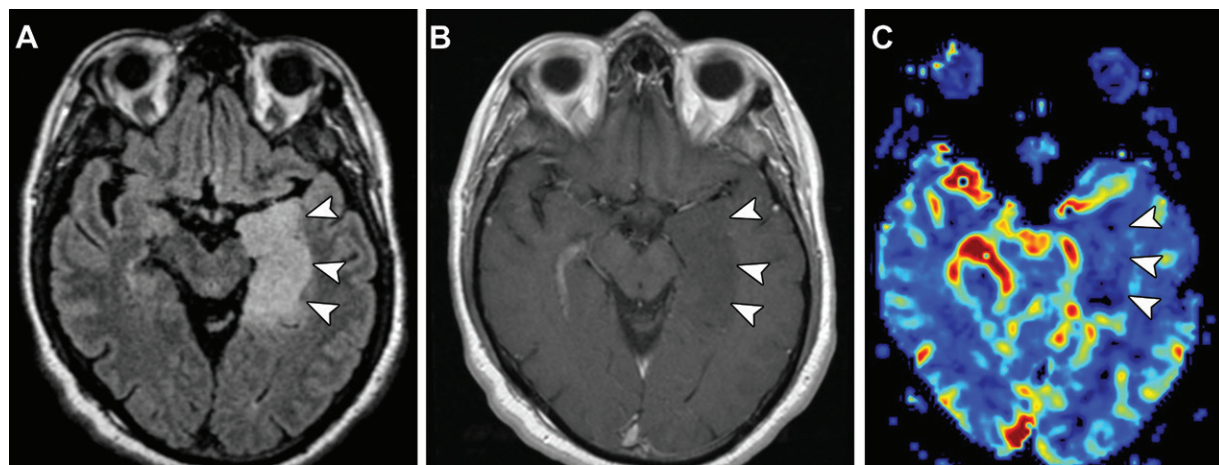
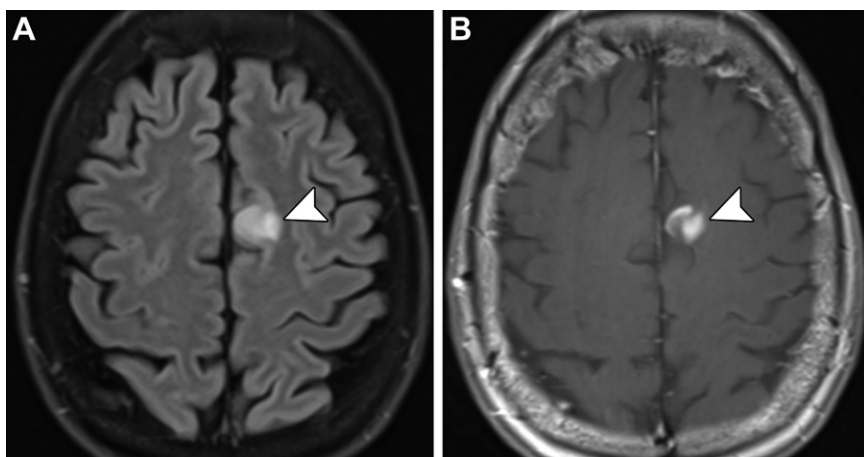


**Figure 4.** *IDH*-wildtype diffuse astrocytic glioma with a molecular feature of glioblastoma (*EGFR* amplification) in a 59-year-old man who presented with seizures. (A) FLAIR MR image shows a hyperintense mass (arrowheads) in the left temporal lobe. (B) On a contrast-enhanced T1-weighted MR image, the mass (arrowheads) does not show contrast enhancement. (C) Dynamic contrast-enhanced susceptibility-weighted perfusion MR image shows the mass (arrowheads) with low relative cerebral blood volume. Although these imaging features suggest a low-grade glioma, given the *EGFR* amplification, the tumor was diagnosed as *IDH*-wildtype glioblastoma, CNS WHO grade 4.

### Molecular, Clinical, and Imaging Features of Newly Recognized CNS Tumor Types

In addition to the major changes in WHO CNS5, multiple newly recognized tumor types (including three provisional types) have been introduced and the nomenclature for some tumor types has been revised (Table, Table E2). As these tumor types are newly recognized, their characteristics are not widely known; thus, literature on the previous classification must be updated (22). In this section, we provide a comprehensive description of the molecular, clinical, and imaging features of these newly recognized CNS tumor types, as classified in WHO CNS5 (Table E2).

#### Pediatric-Type Low-Grade Diffuse Gliomas

*IDH*-wildtype diffuse gliomas in children and young adults were assigned a diagnosis of *IDH*-wildtype or not otherwise specified in the previous

edition of the WHO CNS tumor classification. In WHO CNS5, owing to their distinct clinical appearance, *IDH*-wildtype diffuse gliomas that mainly affect pediatric patients (ie, pediatric diffuse gliomas) are classified separately from *IDH*-wildtype diffuse gliomas that occur in adults (2). Pediatric diffuse gliomas are classified into low- and high-grade groups. The low-grade group includes the following four types: diffuse astrocytoma, *MYB*- or *MYBL1*-altered (CNS WHO grade 1); angiogenic glioma (CNS WHO grade 1); diffuse low-grade glioma, mitogen-activated protein kinase (MAPK) pathway-altered (CNS WHO grade not assigned); and polymorphous low-grade neuroepithelial tumor of the young (PLNTY) (CNS WHO grade 1).

***MYB*- or *MYBL1*-altered Diffuse Astrocytoma and MAPK Pathway-altered Diffuse Low-Grade Glioma.**—Study investigators (6,23,24) have reported indolent clinical behavior with rare

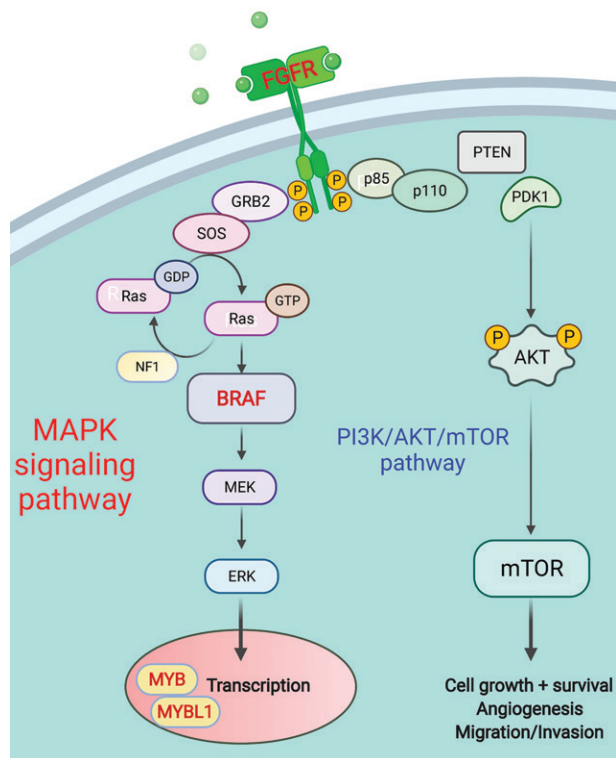


**Figure 5.** Drawing provides a visual depiction of the MAPK signaling pathway and the phosphoinositide 3-kinase/serine-threonine protein kinase/mammalian target of rapamycin (*PI3K/AKT/mTOR*) pathway. Pathogenic alterations in *FGFR*, *BRAF*, or *MYB/MYBL1* induce enhanced cell proliferation and survival, resulting in tumorigenesis (14).

anaplastic progression in *MYB*- or *MYBL1*-altered diffuse astrocytomas and MAPK pathway-altered low-grade astrocytomas. Dominant cases involve pathogenic alterations in *FGFR*, *BRAF*, or *MYB/MYBL1* (Fig 5).

Regarding diffuse astrocytomas, *MYB*- or *MYBL1*-altered, the median age at surgery is reported to be approximately 29 years (range, 4–50 years). In a previous study (25), 24 (92%) of 26 patients reportedly presented with epileptic seizures. Wefers et al (25) reported that diffuse astrocytomas were located in the supratentorial regions in 100% of cases (26 patients). In addition, the tumors typically were hyperintense on T2-weighted fluid-attenuated inversion-recovery (FLAIR) MR images in nine (100%) of nine patients, were hypointense on T1-weighted MR images in eight (100%) of eight patients, had well-defined margins in nine (90%) of 10 patients, and had no contrast enhancement in eight (100%) of eight patients. Most (nine of 11 [81.8%]) of these tumors were larger than 1 cm (25). Six (60%) of ten tumors examined in the study had very sharp margins (25). Conversely, our case described in this review involved linear enhancement (Fig 6). The imaging findings of diffuse low-grade glioma, MAPK pathway-al-

tered, can vary, given the broad spectrum of histologic features, which include astrocytic, oligodendroglial, and mixed features (Fig 7).

### Polymorphous Low-Grade Neuroepithelial Tumor of the Young

—PLNTY is a CNS WHO grade 1 neuroepithelial tumor that mainly affects young (median age, 16 years) and female patients (26). It is characterized by oligodendroglial-like features with extensive expression of CD34 in tumor cells, varying amounts of calcification and cystic components, and genetic alterations in the MAPK pathway (including *FGFR2/3* and *BRAF* alterations) (27). Most patients with PLNTY experience seizures. In a prior study (28), 13 (87%) of 15 patients experienced seizures. A systematic review conducted by our group (28) revealed several imaging characteristics of PLNTY. These characteristics included cortical or subcortical localization (23 [95.8%] of 24 patients) in the temporal lobe (16 [66.7%] of 24 patients), well-delineated tumor margins (16 [72.7%] of 22 patients), calcification (15 [83.3%] of 18 patients), solid and cystic tumor morphology (12 [80.0%] of 15 patients), and scarce or no enhancement (10 [66.7%] of 15 patients) (Fig 8).

In our review (28), a transmantle-like sign (ie, high white matter signal intensity tapering toward the lateral ventricle on T2-weighted or FLAIR MR images) was observed in eight (47.1%) of 17 cases. Three of the eight cases with this sign were associated with pathologically proven focal cortical dysplasia, and the seizure duration was substantially greater in the patients with this sign than in those without it (28).

### Pediatric-Type Diffuse High-Grade Gliomas

In WHO CNS5, pediatric-type diffuse high-grade gliomas were redefined to include the following four types: diffuse midline glioma, *H3 K27-altered*; diffuse hemispheric glioma, *H3 G34-mutant*; diffuse pediatric-type high-grade glioma, *H3-wild-type* and *IDH-wildtype*; and infant-type hemispheric glioma (2).

### Diffuse Hemispheric Glioma, *H3 G34-Mutant*

—Diffuse hemispheric glioma, *H3 G34-mutant*, is a CNS WHO grade 4 tumor characterized by recurrent mutations in the histone gene *H3F3A* (*H3.3*), which result in the substitution of glycine with either arginine or valine at position 34 (G34R/V) (20,21). This tumor type has been found predominantly in young patients with a reported median age of 14–19 years at diagnosis and without a difference in prevalence between males and females (29). Diffuse hemispheric glioma, *H3 G34-mutant*, is known to be

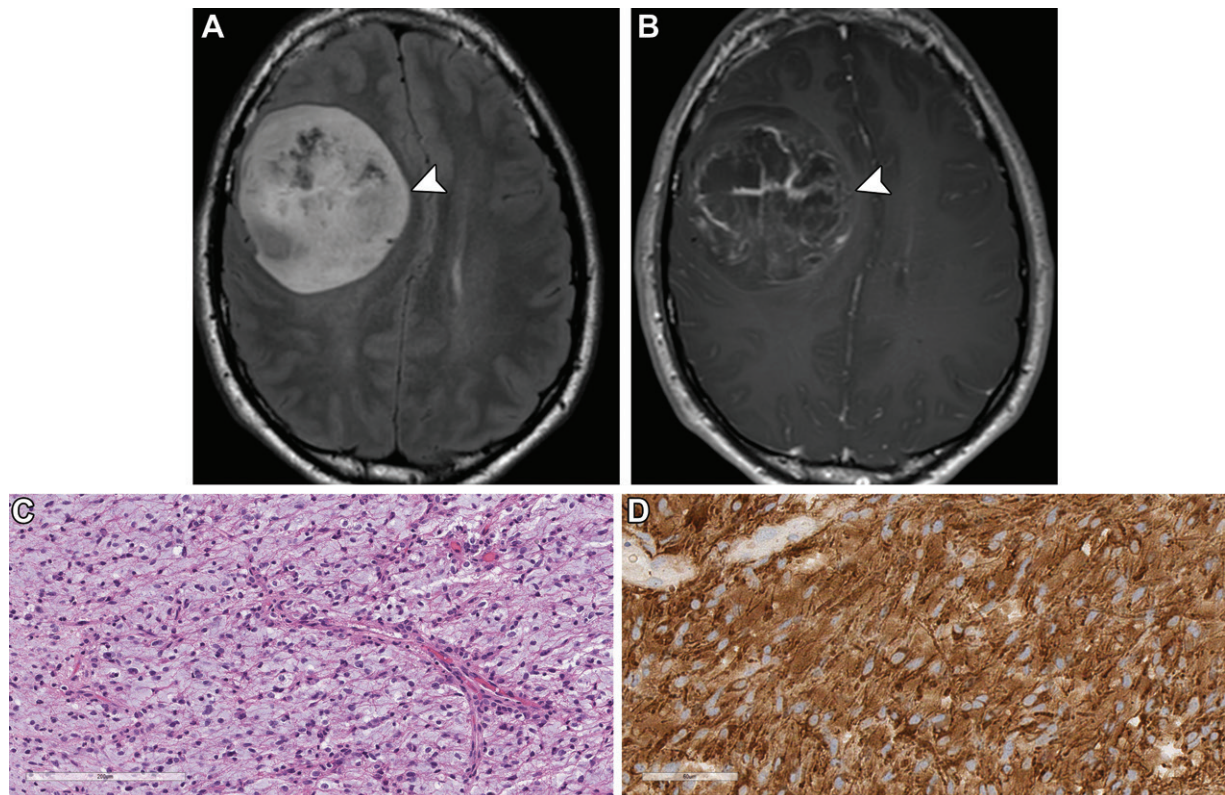
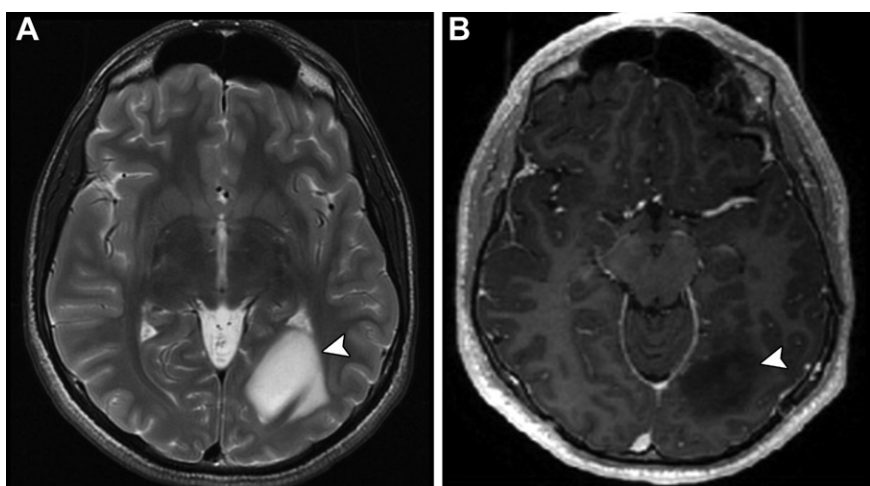


**Figure 6.** Diffuse astrocytoma, *MYB*-altered, in an 18-year-old previously healthy man who had a 12-day history of right-sided sharp headaches and presented with weakness of his left arm. (A, B) Axial T2-weighted FLAIR MR image (A) shows a well-circumscribed mass (arrowhead) in the right frontal lobe, with partial enhancement of the mass on the contrast-enhanced T1-weighted MR image (B). (C) Photomicrograph shows monomorphic glial cells in the strikingly myxoid fibrillar matrix and angiogenic polarity. (Hematoxylin-eosin [H-E] stain; original magnification,  $\times 20$ .) (D) Photomicrograph shows the tumor cells to be diffusely positive for glial fibrillary acidic protein (GFAP) (GFAP immunohistochemical stain; original magnification,  $\times 40$ ), with a very low Ki-67 proliferation index (not shown). No microvascular proliferation or necrosis is seen. No evidence of recurrence was found at 2-year follow-up imaging (not shown).

**Figure 7.** Diffuse low-grade glioma, MAPK pathway-altered, in a 15-year-old boy who presented after a seizure. Axial T2-weighted MR image (A) shows a hyperintense mass (arrowhead) in the left occipital lobe, with no contrast enhancement of the mass on the axial contrast-enhanced T1-weighted MR image (B).



associated with a statistically significantly longer overall survival time (2-year overall survival rate, 27.3%) compared with the overall survival time associated with diffuse midline glioma, *H3 K27*-altered (21.4%) (30).

Histologically, diffuse hemispheric glioma, *H3 G34*-mutant, shows various characteristics,

including glioblastoma-like, anaplastic astrocytoma-like, and primitive neuroectodermal tumor-like features (31). In a systematic review of 59 cases of diffuse hemispheric glioma, *H3 G34*-mutant, our group (29) found that all tumors were localized supratentorially, with predominantly hemispheric localization (35/38 [92.1%]),

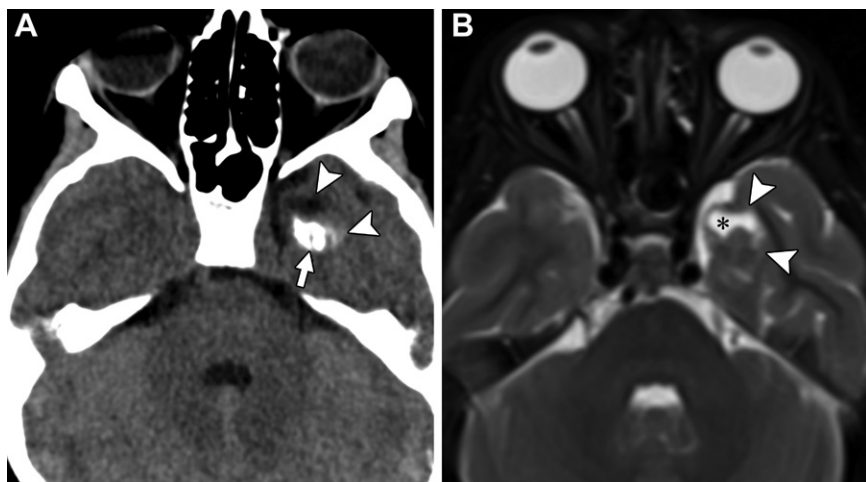


**Figure 8.** PLNTY in a 7-year-old girl with a 1-month history of focal seizure. (A) Axial noncontrast CT image shows a tumor mass (arrowheads) with dense calcification (arrow) in the left temporal lobe. (B) Axial T2-weighted fat-suppressed MR image shows the mass (arrowheads) to have hyperintense areas (\*), indicating cystic components, with involvement of the cortex and subcortex. The tumor demonstrated *FGFR2-CTNNA3* fusion (10q).

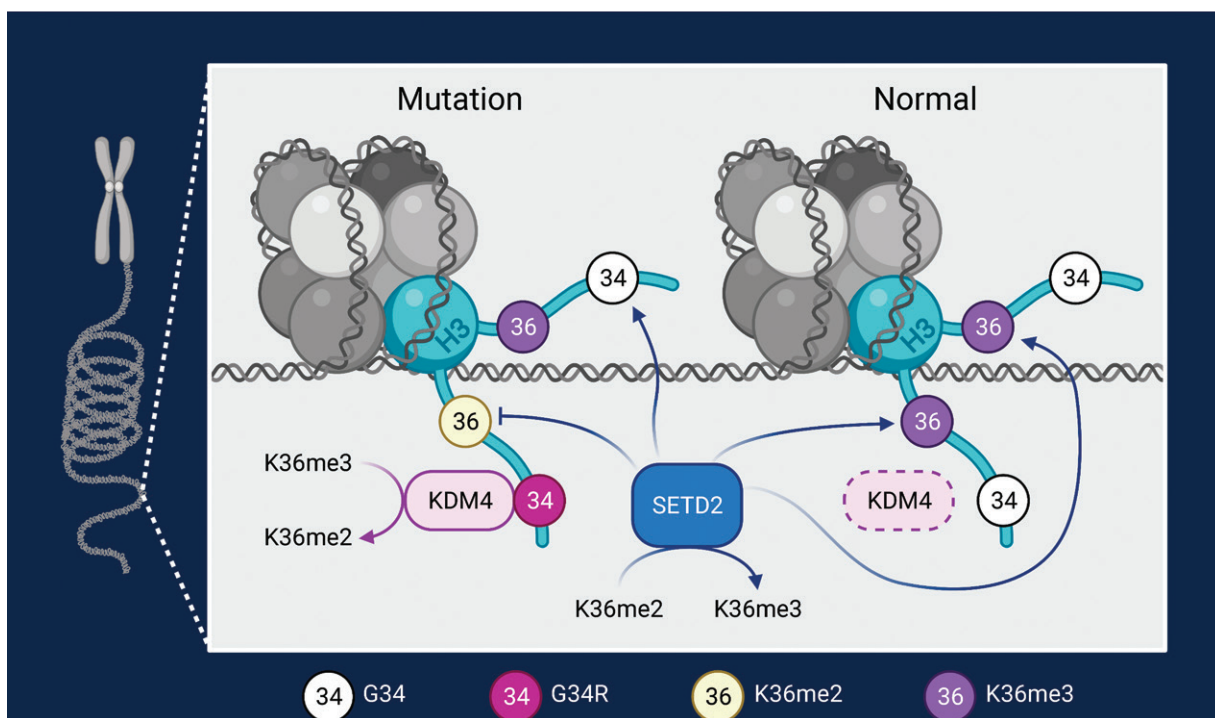


**Figure 9.** Drawing provides a visual depiction of the mechanisms mediating tumorigenesis via G34 mutation (22). Histone H3 gene alterations caused by the substitution of glycine with arginine or valine (G34R/V) at position 34 prevent the recruitment of SET domain-containing 2 (SETD2) methyltransferase, leading to a global decrease in the trimethylation of K36 (K36me3). A global decrease in K36me3 dysregulates DNA mismatch repair, resulting in tumorigenesis.

and most (37/42 [88.1%]) tumors were unifocal. The tumors often showed high attenuation on CT images (8/9 [88.9%]), hyperintensity on T2-weighted (29/35 [82.9%]) and FLAIR (25/25 [100%]) MR images, hypointensity on T1-weighted MR images (12/12 [100%]), diffusion restriction (25/26 [96.2%]), and various patterns of contrast enhancement (42/53 [79.2%]) (Fig 10) (29). This review also revealed that leptomeningeal (36/39 [92.3%]) and ependymal (21/24 [87.5%]) contacts occurred frequently (29). Likewise, intratumoral hemorrhage (19/45 [42.2%]) and cystic and/or necrotic changes

(28/57 [49.1%]) were common (29). MR spectroscopy showed lipid and lactate peaks and an increased choline-to-N-acetylaspartate ratio in seven (58.3%) of 12 patients (29). In this study, patients who had tumors with ill-defined margins reportedly had a statistically significantly shorter survival time compared with those who had tumors with well-delineated margins (29).

**Diffuse Pediatric-Type High-Grade Glioma, H3-Wildtype and IDH-Wildtype.**—Diffuse pediatric-type high-grade gliomas, *H3*-wildtype and *IDH*-wildtype, lack mutations in *H3* and *IDH*

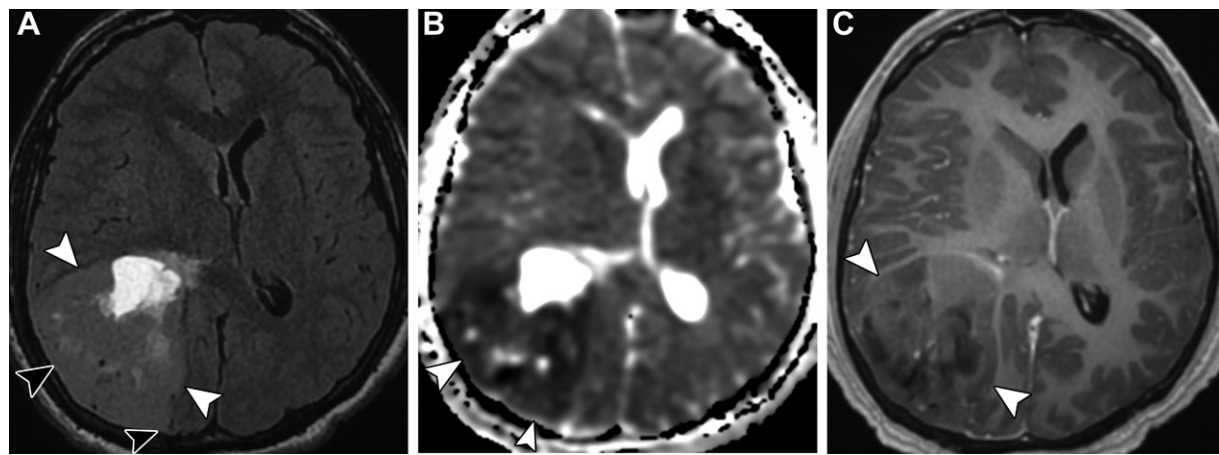


**Figure 10.** Diffuse hemispheric glioma, *H3* G34-mutant (G34R), in a 22-year-old man who presented with an ongoing (1-month duration) headache. (A) Axial FLAIR MR image shows a 64-mm hyperintense tumor mass (white arrowheads) with dural contact (black arrowheads) in the right parietal lobe. (B) Axial apparent diffusion coefficient (ADC) map shows the mass (arrowheads) with an enhancing area, which has a mean ADC of  $0.60 \times 10^{-3}$  mm $^2$ /sec. (C) Axial contrast-enhanced T1-weighted fat-suppressed MR image shows heterogeneous enhancement of the solid component of the mass (arrowheads). The same case was evaluated with different MRI sequences in a prior study (29).

genes. Mackay et al (30) subdivided this group of tumors on the basis of common molecular findings, potentially enabling targeted therapies.

WT-A (wildtype A) tumors are driven by *BRAFV600E* and *NF1* mutations or fusions in *MET*, *FGFR2*, and *NTRK2,3*. This subtype is commonly located in hemispheric areas and was associated with the best overall survival time (median, 38 months) among the three subgroups in the Mackay et al (30) study.

WT-B (wild type B) tumors are unified by chromosome 2 gains and strong upregulation of *MYC* target genes, with amplifications in *EGFR*, *CDK6*, and *MYCN*. Tumors in this group were found in all anatomic compartments and were associated with the poorest overall survival time (median, 14 months).

WT-C (wild type C) tumors are enriched for chromosome 1p and 20q loss mutations and 17q gain mutations, and they harbor amplifications in *PDGFRA* and *MET*. These tumors were found in both hemispheric and midline locations and were associated with a moderate overall survival time (median, 18 months).

In WHO CNS5, the molecular profiles for *EGFR*, *MYCN*, and *PDGFRA* (WT-B and WT-C) were recognized as the key diagnostic findings for integrated CNS tumor classifications (2). In the Mackay et al (30) study, the median age at diagnosis was 12 years (range, 1–30 years), and 30 (42.3%) of the 71 patients enrolled were female. The tumors were located in the hemispheric region in 55 (77.5%) of the 71 patients, in the midline region in 12 (16.9%) patients, and in the brainstem in four (5.6%) patients (30). Other imaging findings have yet to be elucidated; however, heterogeneous masses with variable

enhancement, necrotic and hemorrhagic components, restricted diffusion, increased cerebral blood flow or volume on perfusion-weighted images, and decreased *N*-acetylaspartate levels and increased lactate levels on MR spectroscopic images were observed, as previously reported for pediatric glioblastomas (32).

**Infant-Type Hemispheric Glioma.**—Infant-type gliomas occur in newborns and older infants and have been subdivided into three subgroups with distinct clinical and molecular features (33):

Group 1 (hemispheric, *RTK*-driven) infant-type gliomas harbor *ALK*, *NTRK1/2/3*, *ROS1*, and *MET* alterations and are enriched for high-grade tumors (82.8%). These tumors occur mainly in younger infants (median age at diagnosis, 2.8 months; range, 0–12 months).

Group 2 (hemispheric, *RAS/MAPK*-driven) tumors frequently harbor non-*BRAF RAS/MAPK*-activating alterations and are composed solely of low-grade tumors.

Group 3 (midline, *RAS/MAPK*-driven) usually harbors *BRAF* alterations (97.4%). These tumors are histologically of low grade. Most (79.5%) of the tumors in this group are optic pathway hypothalamic gliomas and primarily (69.2%) pilocytic astrocytomas.

According to WHO CNS5, group 1 infant-type gliomas are newly recognized as infant-type hemispheric gliomas. Knowledge of the imaging features of infant-type hemispheric gliomas currently is limited, although it is likely that most of the high-grade gliomas and glioblastomas previously reported in infants were of this tumor type. Three cases profiled in a study conducted by Guerreiro Stucklin et al (33) involved large

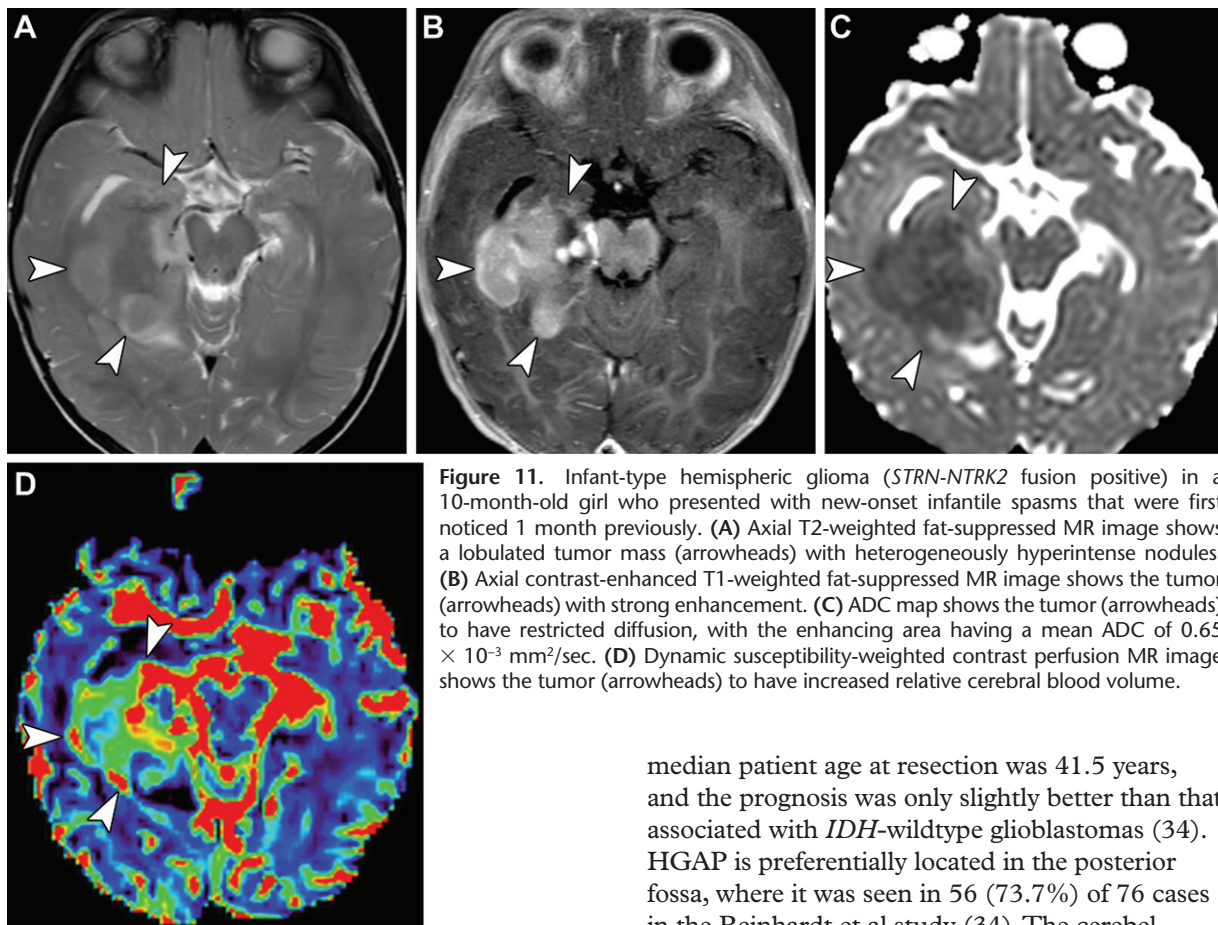


**Figure 11.** Infant-type hemispheric glioma (*STRN-NTRK2* fusion positive) in a 10-month-old girl who presented with new-onset infantile spasms that were first noticed 1 month previously. (A) Axial T2-weighted fat-suppressed MR image shows a lobulated tumor mass (arrowheads) with heterogeneously hyperintense nodules. (B) Axial contrast-enhanced T1-weighted fat-suppressed MR image shows the tumor (arrowheads) with strong enhancement. (C) ADC map shows the tumor (arrowheads) to have restricted diffusion, with the enhancing area having a mean ADC of  $0.65 \times 10^{-3} \text{ mm}^2/\text{sec}$ . (D) Dynamic susceptibility-weighted contrast perfusion MR image shows the tumor (arrowheads) to have increased relative cerebral blood volume.

lobulated hemispheric tumors with solid nodules and cystic or necrotic components. Non-contrast CT depicted intratumoral hemorrhage in one patient.

In one of our cases, the solid nodules of the tumor showed diffusion restriction and increased perfusion (Fig 11). In this particular case, larotrectinib (ie, tropomyosin receptor kinase inhibitor) treatment was administered, given the *STRN-NTRK2* fusion of the tumor.

### Circumscribed Astrocytic Gliomas

According to WHO CNS5, circumscribed astrocytic gliomas include pilocytic astrocytomas; high-grade astrocytomas with piloid features (HGAP); pleomorphic xanthoastrocytomas; subependymal giant cell astrocytomas; chordoid gliomas; and astroblastomas, *MN1*-altered (2).

### High-Grade Astrocytomas with Piloid Features

HGAP is defined according to a specific DNA methylation profile. Reinhardt et al (34) retrospectively investigated the DNA methylation status of 102 histologically defined anaplastic pilocytic astrocytomas and found that 83 (81.4%) tumors formed a specific DNA methylation group. The

median patient age at resection was 41.5 years, and the prognosis was only slightly better than that associated with *IDH*-wildtype glioblastomas (34). HGAP is preferentially located in the posterior fossa, where it was seen in 56 (73.7%) of 76 cases in the Reinhardt et al study (34). The cerebellum is the most common location (48 [63.2%] of 76 cases in the Reinhardt et al study), with the supratentorial region (13 [17.1%] of 76 cases in the Reinhardt et al study) being the second most common site (34).

Bender et al (35) reported six cases of HGAP imaged with MRI, including two cases involving the spinal cord, and found a tendency toward a lack of central enhancement (Fig 12). HGAP showed hyperintensity on T2-weighted MR images (in six [100%] of six cases) and hypo- or isointensity on noncontrast T1-weighted MR images (in six [100%] of six cases), as well as a lack of diffusion restriction (in three [100%] of three cases) and heterogeneous contrast enhancement (in five [83.3%] of six cases). Sharp tumor margins and surrounding edema were observed in four (66.7%) of the six profiled cases, and necrosis was observed in one (16.7%) case (35). Increased tracer uptake was observed at *O*-(2-[<sup>18</sup>F]fluoroethyl)-*l*-tyrosine (FET) PET in two (100%) of two cases (35).

### Glioneuronal and Neuronal Tumors

In WHO CNS5, glioneuronal and neuronal tumors are defined to include ganglioglioma, desmoplastic infantile ganglioglioma and astrocytoma, dysembryoplastic neuroepithelial tumor, diffuse glioneuronal tumor with oligodendrogioma-like features and nuclear clusters (provisional type),

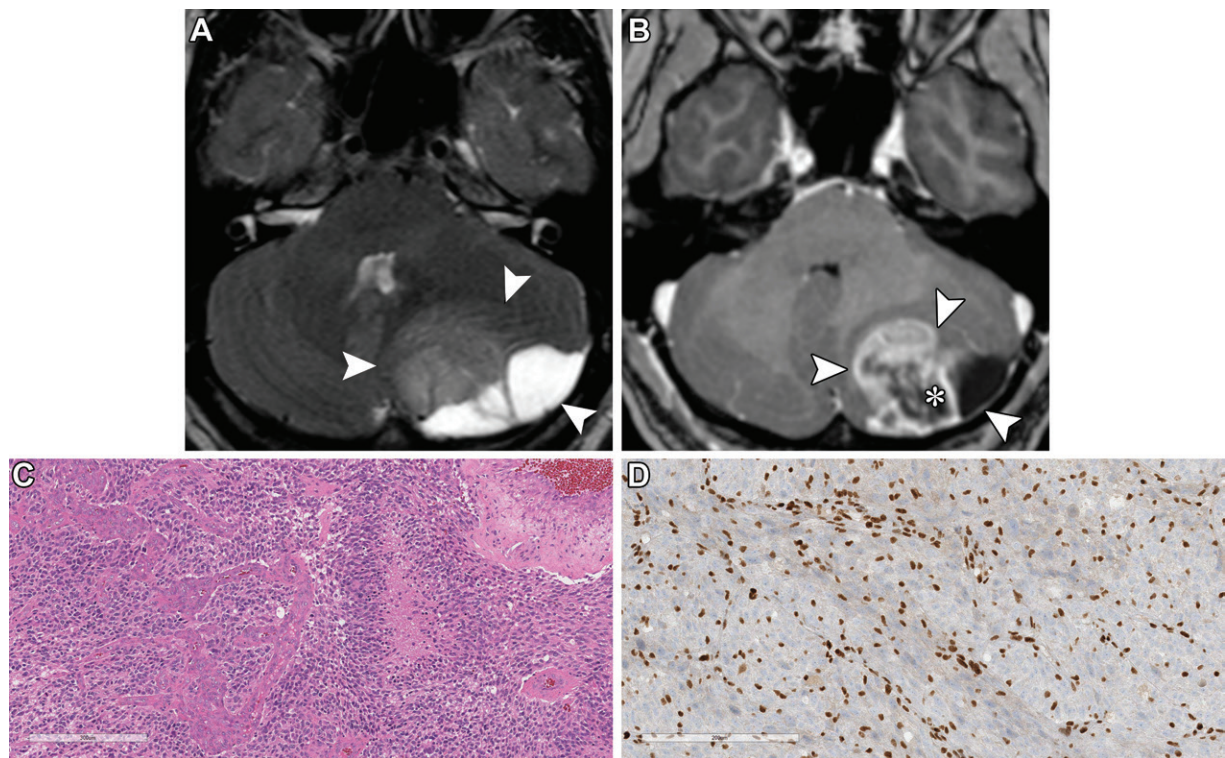


**Figure 12.** HGAP in a 41-year-old man who presented with progressive headaches, nausea, and vomiting. (A, B) MR images show a solid and cystic tumor mass (arrowheads) with a relatively well-defined margin in the left cerebellar hemisphere. The tumor has heterogeneous hyperintensity on the T2-weighted fat-suppressed image (A) and heterogeneous enhancement with a lack of central enhancement (\*) in B on the contrast-enhanced T1-weighted fat-suppressed image (B), without diffusion restriction (not shown). (C, D) Photomicrographs show microvascular proliferation and numerous mitotic figures (H-E stain; original magnification,  $\times 20$ ) (C), with alpha thalassemia-mental retardation syndrome X-linked (ATRX) protein lost in tumor cells (ATRX immunohistochemical stain; original magnification,  $\times 20$ ) (D).

papillary glioneuronal tumor, rosette-forming glioneuronal tumor, myxoid glioneuronal tumor, gangliocytoma, multinodular and vacuolating neuronal tumor (MVNT), dysplastic cerebellar gangliocytoma (ie, Lhermitte-Duclos disease), central neurocytoma, extraventricular neurocytoma, and cerebellar liponeurocytoma (2).

### Myxoid Glioneuronal Tumors

Myxoid glioneuronal tumors are slow-growing glioneuronal tumors associated with favorable clinical outcomes, and they are most frequently centered in the septum pellucidum (36). In a prior study (36), the median patient age at surgery was 23.6 years (range, 6–65 years), and the presenting symptoms were variable and included intermittent headaches and subjective cognitive disturbance. Myxoid glioneuronal tumors are histologically characterized by oligodendrocyte-like tumor cells with an abundant myxoid or mucin-rich stroma. Genetically, myxoid glioneuronal tumors are characterized by recurrent dinucleotide substitutions that result in K385 L/I mutations in *PDGFRA* (37). Narvaez et al (38) summarized the MRI findings of myxoid glioneuronal tumors in three cases and reported that they

are typically well-defined lobulated masses with strong hyperintensity on T2-weighted images, hypointensity on T1-weighted images, and no contrast enhancement or diffusion restriction. Narvaez et al (38) emphasized the importance of obtaining FLAIR MR images, which showed signal suppression in the center of the tumors (ie, T2-FLAIR mismatch sign), with a hyperintense peripheral rim (Fig 13).

### Multinodular and Vacuolating Neuronal Tumor

MVNT is a clinically benign neuroepithelial tumor type (CNS WHO grade 1) that was described in the previous WHO CNS classification, in the commentary on ganglion cell tumors, as a histopathologic pattern. Although there has been some debate as to whether MVNT is a genuine tumor, given the specialized glial antigen expression of MVNT cells, it is now recognized as one of the new glioneuronal and neuronal tumors in WHO CNS5, as mentioned earlier (2). Genetically, MVNTs are negative for *BRAF* mutations and for abnormalities involving *IDH1/2*, *ATRX*, *TP53*, *TERT*, *CIC*, *FUBP1*, *PRKCA*, *CDKN2A*, and *FGFR1*.

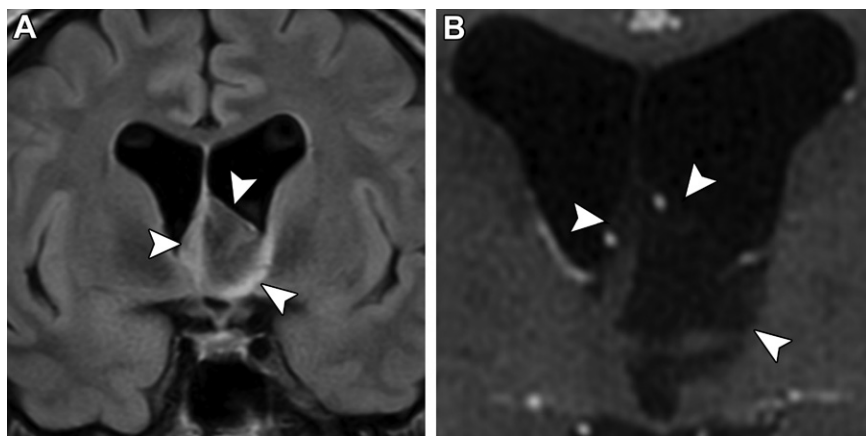


**Figure 13.** Myxoid glioneuronal tumor in a 33-year-old woman who presented with photophobia and morning headaches. MR images show an intraventricular mass (arrowheads) attaching to the septum pellucidum and thereby causing hydrocephalus, with signal suppression in the center of the tumor on the coronal FLAIR image (A), as compared with the signal intensity seen on T2-weighted MR images (not shown), and a peripheral rim of hyperintensity (A). No contrast enhancement is observed on the coronal contrast-enhanced image (B).

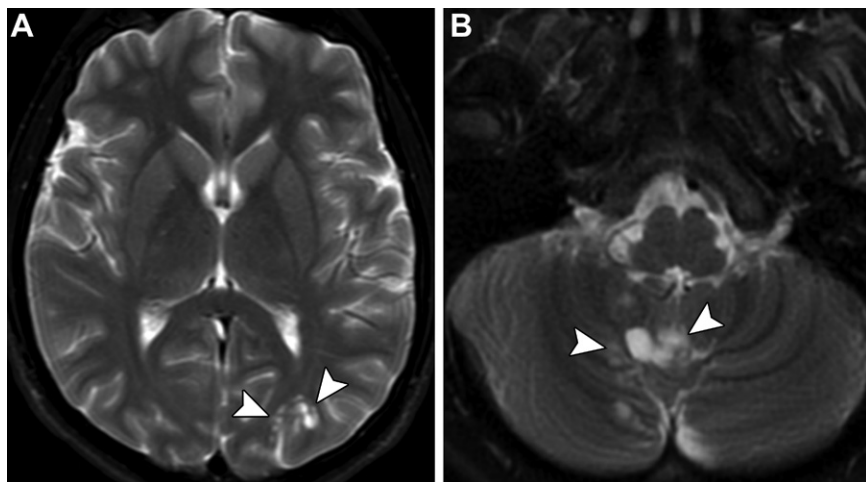


**Figure 14.** MVNT in a 19-year-old man and multinodular and vacuolating posterior fossa lesions of unknown significance (MV-PLUS) in a 36-year-old woman. On T2-weighted fat-suppressed MR images, both MVNT (arrowheads in A) and MV-PLUS (arrowheads in B) show a cluster of well-circumscribed "bubbly" hyperintensity, without contrast enhancement (not shown).

(8). However, genetic alterations that activate the MAPK signaling pathway have been identified in MVNT (39). In a previous study (40), the mean patient age at diagnosis was 42 years (range, 16–77 years), with a female-to-male ratio of 2.2:1.0. MVNT frequently involves the deeper cortical layers and the subjacent white matter of the supratentorial regions, with the frontal and temporal lobes being the most common sites (Fig 14A) (41).

Nunes et al (41) reported MRI findings of MVNT that included hyperintensity on FLAIR (33 [100%] of 33 cases) and T2-weighted (33 [100%] of 33 cases) images, mild hypo- or isointensity on T1-weighted images (29 [87.9%] of 33

cases), and abnormal white matter signal intensity surrounding cortical and subcortical bubble-like lesions (15 [45.5%] of 33 cases). Contrast enhancement was observed in one (3.0%) case, and no diffusion restriction or blooming was found on susceptibility-weighted MR images (41).

Some authors (42–44) have reported posterior fossa lesions with imaging patterns similar to those of MVNT; Lecler et al (42) named these entities multinodular and vacuolating posterior fossa lesions of unknown significance (MV-PLUS) (42–44). However, given the lack of a well-defined molecular profile for these lesions, it is unclear whether MV-PLUS (Fig 14B) represents a rare pattern of MVNT.

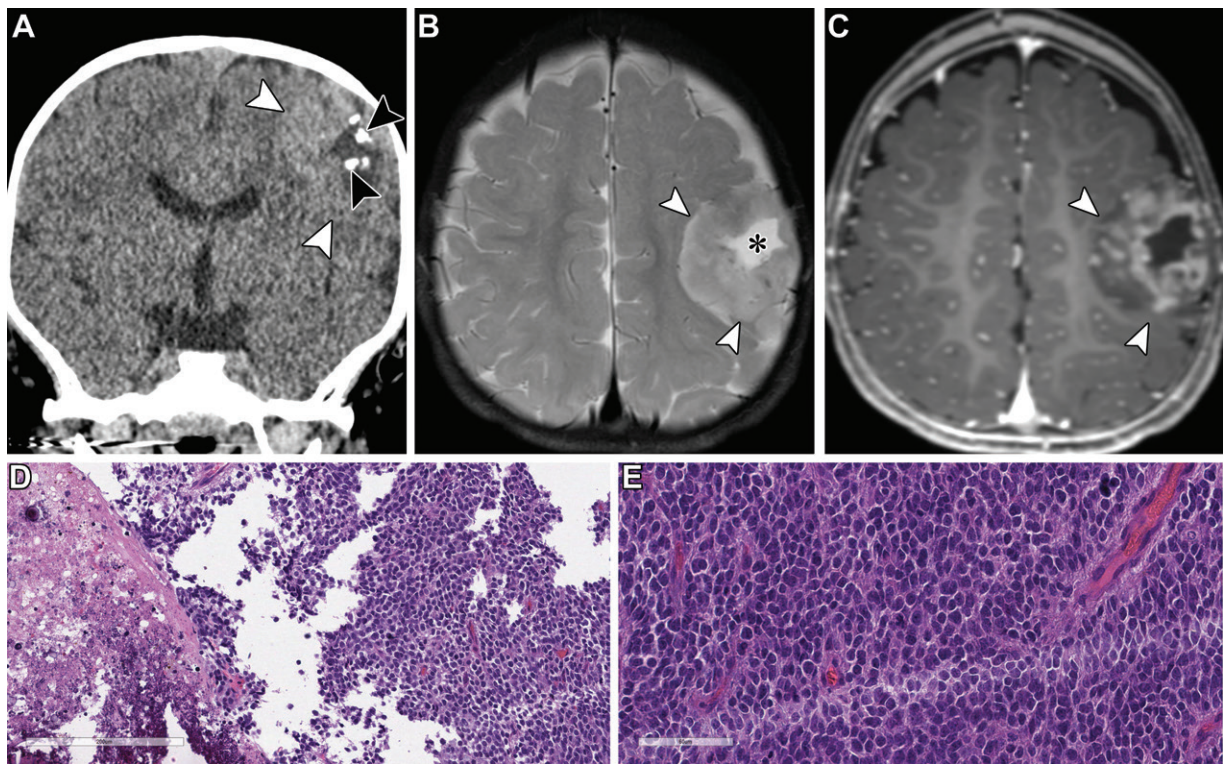


**Figure 15.** CNS neuroblastoma, *FOXR2*-activated, in a 19-month-old girl who presented with refractory epileptic seizures. (A) Coronal noncontrast CT image shows a hyperattenuating, lobulated, solid and cystic mass (white arrowheads) with calcifications (black arrowheads) along the inner rim. (B) Axial T2-weighted MR image shows a hyperintense tumor (arrowheads) with a central cystic component (\*). (C) Axial contrast-enhanced T1-weighted fat-suppressed MR image shows wavy contrast enhancement inside and poor enhancement outside the tumor (arrowheads). The tumor demonstrated restricted diffusion, with a mean ADC of  $0.74 \times 10^{-3}$  mm $^2$ /sec (not shown). (D) Photomicrograph shows a densely cellular tumor with small to medium-sized cells and hyperchromatic nuclei. (H-E stain; original magnification,  $\times 20$ .) (E) Photomicrograph shows areas of necrosis and numerous mitotic figures. (H-E stain; original magnification,  $\times 40$ .) The tumor cells are diffusely positive for synaptophysin, with a high Ki-67 proliferation index (40%–60%) (not shown).

### Other CNS Embryonal Tumors

As defined in WHO CNS5, other CNS embryonal tumors include atypical teratoid or rhabdoid tumors; *cribriform neuroepithelial tumors (provisional type)*; embryonal tumors with multilayered rosettes; CNS neuroblastomas, *FOXR2*-activated; CNS tumors with *BCOR* internal tandem duplication (CNS-*BCOR* ITD); and CNS embryonal tumors. The “other” in this group refers to CNS embryonal tumors other than medulloblastomas (2).

### CNS Neuroblastoma, *FOXR2*-activated

CNS neuroblastomas, *FOXR2*-activated, are embryonal tumors with a primitive neuronal architecture and/or neurocytic differentiation and are characterized by the activation of the *FOXR2* transcription factor (45). CNS neuroblastomas, *FOXR2*-activated, are usually found in children younger than 10 years. The imaging characteristics of these tumors have been poorly characterized thus far. However, in a case series reported by Holsten et al (46), MRI depicted large supratentorial solid and cystic masses of high cellularity with or without contrast enhancement. Moreover, in representative descriptions of this tumor type,

Furuta et al (45) reported that noncontrast CT depicted a lobulated solid and cystic mass with isoattenuation (compared with the attenuation of the cortex). Intratumoral calcification along the inner rim was observed in a case described by Furuta et al and in one of our cases (Fig 15).

### CNS Tumors with *BCOR* Internal Tandem Duplication

CNS-*BCOR* ITD is a malignant neoplasm with a somatic internal tandem duplication at the 3' end (exon 15) of the *BCOR* gene. CNS-*BCOR* ITD usually affects children younger than 10 years and is associated with a poor overall survival; however, the overall evidence is not definitive, given the limited number of reported cases to date (47). Cardoen et al (48) reported imaging findings in 10 cases of CNS-*BCOR* ITD and found the tumors to be large (4.7–9.2-cm) well-defined intraparenchymal masses in the cerebral or cerebellar hemispheres. These features were consistent with those in a series of five cases reported on by Yoshida et al (47). The tumors had slightly higher signal intensity than the normal gray matter on T2-weighted MR

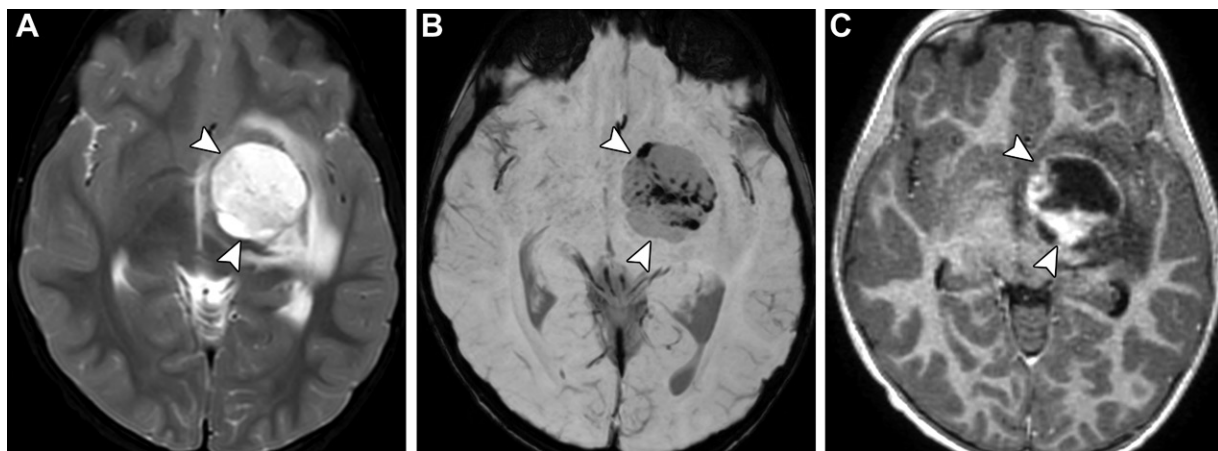


**Figure 16.** *CIC*-rearranged sarcoma (*ATXN1-DUX4* fusion) in a 3-year-old boy. The same case was evaluated with different MRI sequences in a prior study (52). Axial MR images show a 3.5-cm tumor (arrowheads) with a well-defined margin and surrounding edema, in the left basal ganglia. (A) T2-weighted fat-suppressed MR image shows the tumor with heterogeneous hyperintensity and cystic components. (B) Susceptibility-weighted MR image shows susceptibility artifact, indicating intratumoral hemorrhage. (C) Contrast-enhanced T1-weighted MR image shows homogeneous enhancement of the solid components of the tumor.

images and hypointensity on T1-weighted MR images (48). In 10 cases of CNS-BCOR ITD in the Cordeon et al (48) study, necrosis (nine [90.0%] cases), hemorrhage (eight [80.0%] cases), calcification (four [57.1%] cases), diffusion restriction (10 [100%] cases), mild and heterogeneous enhancement at MRI or CT (10 [100%] cases), large intratumoral macroscopic vessels connected to cortical veins (nine [90.0%] cases), and absence of peritumoral edema (10 [100%] cases) were reported.

### Pineal Tumors

In WHO CNS5, pineal tumors include pineocytomas; pineal parenchymal tumors of intermediate differentiation; pineoblastomas; papillary tumors of the pineal region; and desmoplastic myxoid tumors of the pineal region, *SMARCB1*-mutant (2).

### Desmoplastic Myxoid Tumors of the Pineal Region, *SMARCB1*-Mutant

Desmoplastic myxoid tumors of the pineal region, *SMARCB1*-mutant, are rare pineal tumors with *SMARCB1* mutation (49). In one study (49), the median age of patients with these tumors was 40 years (range, 15–61 years), and all tumors were located in the pineal region. Despite having epigenetic similarities with atypical teratoid and rhabdoid tumors, desmoplastic myxoid tumors of the pineal region, *SMARCB1*-mutant, lack histopathologic signs of malignancy and are associated with moderate prognoses (49). The imaging features of this tumor type are yet to be established. In a case reported by Wang et al (50), these tumors were found to have high attenuation on noncontrast CT images, isointensity relative to the cortex on T2-weighted MR images, and central calcification. In a case reported by Matsu-

mura et al (51), the desmoplastic myxoid tumor of the pineal region, *SMARCB1*-mutant, was a hemorrhagic pineal mass with hypointensity on T1-weighted MR images, isointensity on T2-weighted MR images, and contrast enhancement.

### Soft-Tissue Tumors with Uncertain Differentiation

In WHO CNS5, soft-tissue tumors with uncertain differentiation (ie, mesenchymal nonmeningotheelial tumors) include *intracranial mesenchymal tumors*, *FET-CREB* fusion-positive (provisional type); *CIC*-rearranged sarcomas; primary intracranial sarcomas, *DICER1*-mutant; and Ewing sarcomas (2).

### *CIC*-rearranged Sarcoma

*CIC*-rearranged sarcoma is a molecularly characterized mesenchymal malignant tumor with a translocation involving *CIC* located on chromosome 19. The most common fusion partner in extra-CNS *CIC*-rearranged sarcoma is *DUX4*; less common partners include *NUTM1*, *NUTM2A*, *FOXO4*, and *LEUTX* (52). In contrast, *CIC*-rearranged sarcomas of the CNS more commonly involve *NUTM1*. The median age of affected patients reported in prior studies was 23 years (range, 3–64 years) (52,53). *CIC*-rearranged sarcoma is usually refractory to chemotherapy, and compared with Ewing sarcoma, it is associated with a statistically significantly worse overall survival. A comprehensive understanding of the imaging features is yet to be established. However, in our experience, intratumoral hemorrhage and cystic changes are frequently observed. The reported cases have involved masses that are large at diagnosis and tend to have at least partially well-defined margins (Fig 16). Pratt et al (52) recently reported the first case

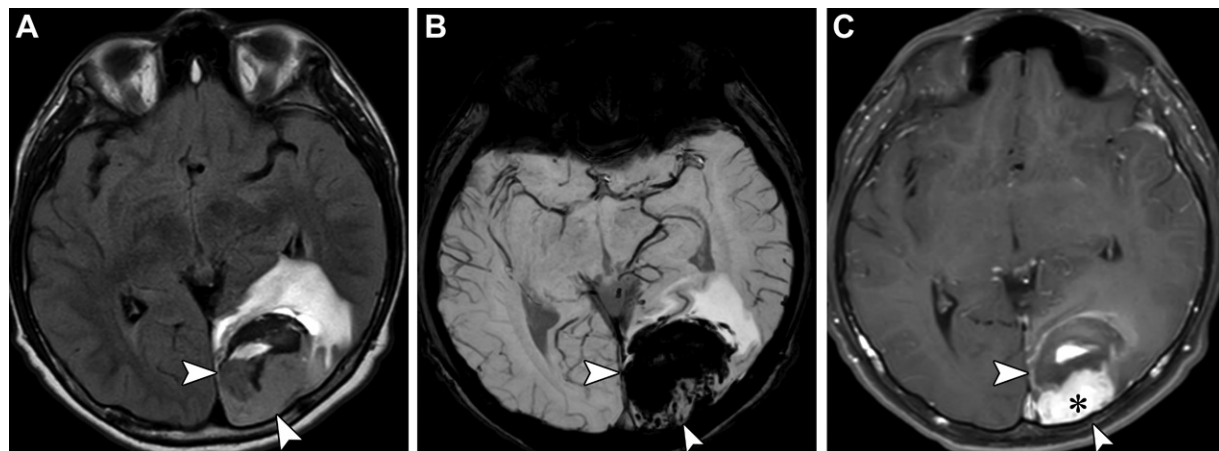


**Figure 17.** Primary intracranial sarcoma, *DICER1*-mutant, in a 12-year-old boy with no prior medical history of note, who presented with an acute-onset headache. Axial MR images show a 5-cm tumor (arrowheads) attaching to the dura in the left occipital lobe, with surrounding edema. (A) FLAIR image shows the tumor to have mild hyperintensity. (B) Susceptibility-weighted image shows susceptibility artifact that is indicative of intratumoral hemorrhage. (C) Contrast-enhanced T1-weighted fat-suppressed image shows homogeneous enhancement (\*) of the solid components of the tumor.

of cerebral *CIC*-rearranged sarcoma with non-*CIC* fusion (ie, *ATXN1-DUX4* fusion), potentially expanding the spectrum of this tumor type.

### Primary Intracranial Sarcoma, *DICER1*-Mutant

*DICER1* encodes dicer, an RNase III endonuclease that is responsible for the cleavage of miRNA precursors (54). Dysfunction of dicer leads to abnormal expression of genes that are regulated by mature microRNAs and subsequent abnormalities in organogenesis and cell proliferation, resulting in tumorigenesis. Primary CNS tumors associated with *DICER1* mutations include primary intracranial sarcomas, *DICER1*-mutant; pineoblastomas; pituitary blastomas; ciliary body medulloepitheliomas; and embryonal tumors with multilayered rosette-like infantile cerebellar tumors (55). Tumors associated with *DICER1* mutations manifest as familial *DICER1* syndrome, a pleiotropic tumor predisposition syndrome that is mainly caused by inherited germline loss-of-function mutations of *DICER1*, or as sporadic tumors with two somatic *DICER1* variants.

Regarding primary intracranial sarcoma, *DICER1*-mutant, the median patient age at diagnosis is 6 years (range, 2.1–13.6 years) with no obvious male versus female difference; the median overall survival time after the diagnosis is 1.7 years (range, 0.1–5.0 years) (56). Primary intracranial sarcomas, *DICER1*-mutant, are located predominantly in the frontal or parietal lobes, with one reported case arising in the cerebellum (56). These tumors are typically large, with at least partially well-defined margins, and intratumoral hemorrhage occurs quite frequently (Fig 17) (56).

### Tumors of the Sellar Region

In WHO CNS5, tumors of the sellar region include adamantinomatous craniopharyngiomas, papillary craniopharyngiomas, pituicytomas, granular cell tumors of the sellar region, spindle cell oncocyomas, pituitary adenoma and pituitary neuroendocrine tumors, and pituitary blastomas (2).

### Pituitary Blastoma

Pituitary blastomas are anterior hypophyseal tumors that mainly affect infants younger than 24 months and are considered pathognomonic features of *DICER1* syndrome (57). According to the diagnostic criteria summarized by Liu et al (58), the symptoms of 17 patients after presentation included Cushing syndrome (10 [58.8%] patients), cranial nerve palsy (seven [41.2%] patients), reduced visual acuity (four [23.5%] patients), developmental delays (four [23.5%] patients), and intracranial hypertension-associated symptoms (three [17.6%] patients). The tumor sizes in previously reported cases have varied from 1.7 to 12.0 cm (58).

The imaging features of pituitary blastomas are yet to be established. In two cases evaluated with MRI in a study by de Kock et al (57), an intra- and suprasellar isointense mass was seen on T1- and T2-weighted images (with multiple internal cystic components) in one case, and an intra- and suprasellar heterogeneously enhanced mass was seen in the other case. Lobulated intra- and suprasellar heterogeneously enhanced masses with single or multiple cystic components were also observed in cases reported by Scheithauer et al (59) and Chhuon et al (60). Other frequently observed imaging findings include compression of the optic chiasm and tumor extension into the cavernous sinus.

## Ependymal Tumors

In WHO CNS5, ependymal tumors include supratentorial ependymomas; supratentorial ependymomas, *ZFTA* fusion-positive; supratentorial ependymomas, *YAP1* fusion-positive; posterior fossa ependymomas; posterior fossa ependymomas, group PFA (posterior fossa group A); posterior fossa ependymomas, group PFB (posterior fossa group B); spinal ependymomas; spinal ependymomas, *MYCN*-amplified; myxopapillary ependymomas; and subependymomas (2).

### Supratentorial Ependymoma, *YAP1* Fusion-Positive

*YAP1* (yes-associated protein 1) is a transcriptional cofactor that functions as a key effector of the Hippo tumor suppressor pathway. A characteristic fusion between *YAP1* and *MAMLD1* leads to transcription activation, resulting in tumorigenesis of a group of supratentorial ependymomas (Fig 18) (61).

According to a summary by Andreiuolo et al (61), the median age at onset of supratentorial ependymomas, *YAP1* fusion-positive, is 8.2 months (range, 4.8–175.0 months) with a female predominance (13 [86.7%] of 15 patients), and the prognosis for patients with supratentorial ependymomas, *YAP1* fusion-positive, is more favorable than that for those with supratentorial ependymomas, *RELA* fusion-positive. In the Andreiuolo et al (61) study, the tumor was larger than 5 cm in eight (100%) of eight cases, and intra- and paraventricular locations were quite frequent (in nine [90%] of 10 cases).

In the Andreiuolo et al (61) study, supratentorial ependymomas, *YAP1* fusion-positive, typically had both solid and cystic components (nine [90.0%] of 10 cases); were iso- to hypointense compared with the cortex on T2-weighted MR images (nine [100%] of nine cases), isointense on T1-weighted MR images (eight [88.9%] of nine cases), and iso- to hypointense on ADC maps (seven [100%] of seven cases); and had ring enhancement (eight [80.0%] of 10 cases). There were no cases of infiltrative growth patterns at the tumor margins (61).

### Posterior Fossa Ependymoma, Group PFA and Group PFB

Posterior fossa ependymomas are subdivided into two main groups, PFA and PFB, which are delineated on the basis of DNA methylation profiles and/or the immunohistochemical loss (PFA) or retention (PFB) of nuclear *H3 K27me3* expression (9). These subgroups are known to show distinct clinical features.

According to data in one study (62), group PFA tumors mainly affect children up to 8 years

of age (224 [93.3%] of 240 patients; median age, 3 years [range, 0–51 years]), with a male predominance (154 [64.2%] of 240 patients). Group PFA posterior fossa ependymomas are associated with unfavorable outcomes, with a 5-year overall survival rate of 68%, as compared with the 5-year overall survival rate of 100% for the PFB group (62). According to data in the Pajtler et al (62) study, posterior fossa ependymoma, group PFB, typically occurs in adults (median age, 30 years; age range, 10–65 years), with a mild female predominance (30 [58.8%] of 51 patients).

Yonezawa et al (63) reported the radiologic features of posterior fossa ependymomas (both group PFA and group PFB) and found that tumor extension beyond the fourth ventricle (five [55.6%] of nine versus two [28.6%] of seven cases) and calcification (six [66.7%] of nine versus one [14.3%] of seven cases) occurred more frequently in the PFA group than in the PFB group. They also reported that the PFB group tended to have a larger contrast-enhanced area compared with the PFA group (mean enhanced area, 79.79% vs 46.69%) (Figs 19, 20) (63).

### Spinal Ependymoma, *MYCN*-amplified

*MYCN* is a proto-oncogene in the *MYC* gene family that encodes the transcription factor *N-MYC*. *MYCN* amplification and the subsequent abnormal expression of *N-MYC* are known to be associated with tumorigenesis (eg, neuroblastomas, retinoblastomas, gliomas) and are associated with poor prognoses (64).

Spinal ependymoma, *MYCN*-amplified, typically involves the cervical and/or thoracic spinal cord with frequent concomitant leptomeningeal disease, as seen in 50% (four of eight) of cases in one study (65). Based on prior research (65), the median patient age at diagnosis is 35.5 years (range, 24–52 years), with no sex-based preference. Swanson et al (66) reported on two cases evaluated with MRI: One case involved an intra- and extramedullary mass with isointensity on T1-weighted images, hyperintensity with small cystic areas at the top and bottom of the tumor on T2-weighted images, and homogeneous enhancement with peritumoral edema in the cervical region. The other case was that of multiple intradural, extramedullary enhanced nodules along the thoracic spinal cord.

## Provisional Tumor Types

Three newly recognized provisional tumor types were introduced in WHO CNS5: *diffuse glioneuronal tumors with oligodendrogloma-like features and nuclear clusters*; *cryptocystic neuroepithelial tumors*; and *intracranial mesenchymal tumors, FET-CREB fusion-positive* (Fig 21) (2). These

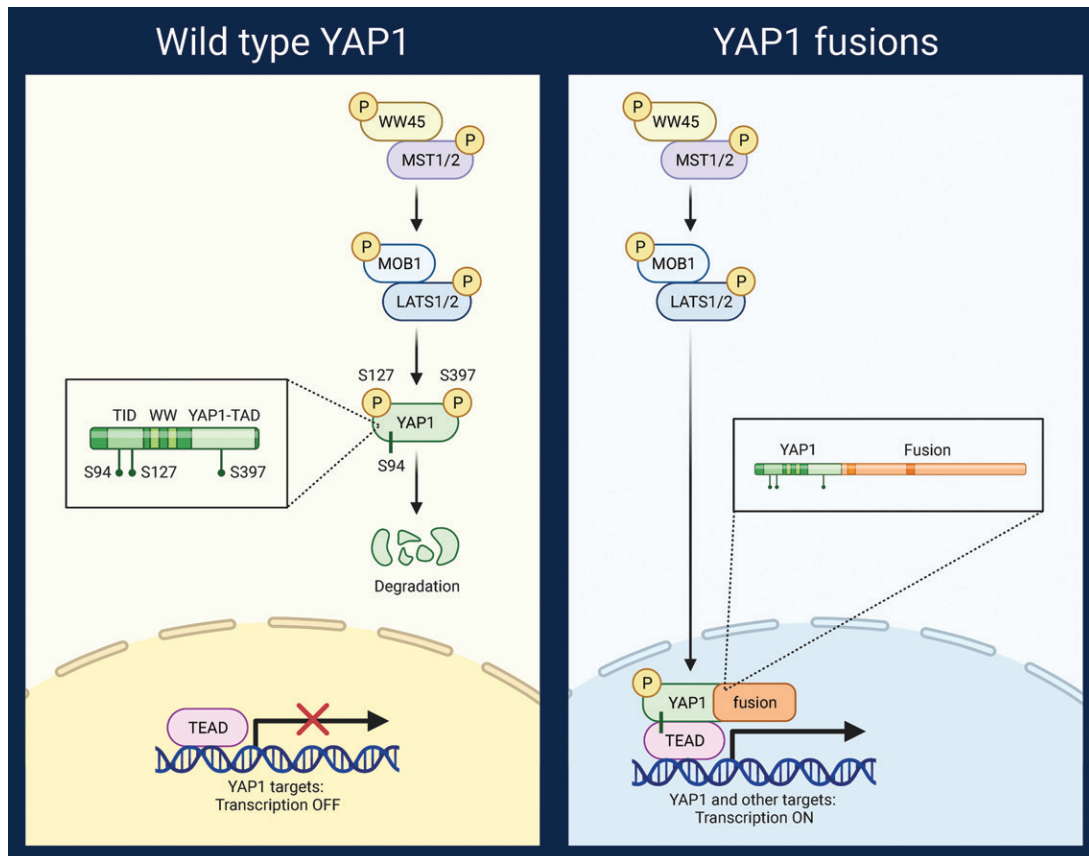


**Figure 18.** Drawings provide visual depictions of the Hippo tumor suppressor pathway with *YAP1* fusion. Wildtype *YAP1* is regulated by the Hippo tumor suppressor pathway (left). When a fusion is formed between *YAP1* and partner genes, the transcription becomes activated, thereby leading to tumorigenesis (right).

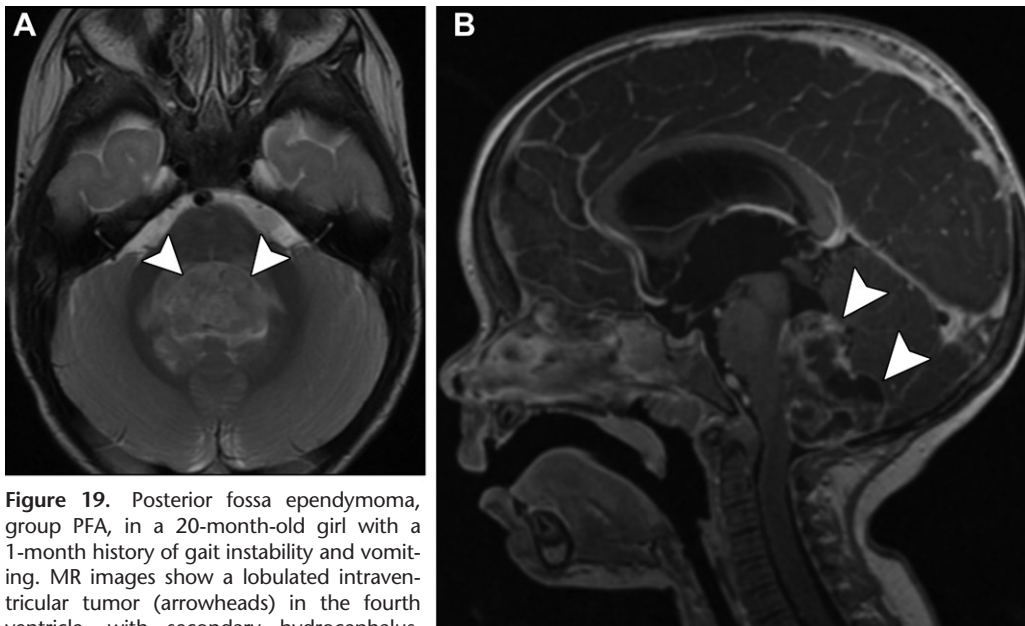


**Figure 19.** Posterior fossa ependymoma, group PFA, in a 20-month-old girl with a 1-month history of gait instability and vomiting. MR images show a lobulated intraventricular tumor (arrowheads) in the fourth ventricle, with secondary hydrocephalus. (A) Axial T2-weighted image shows the tumor to have heterogeneous signal intensity with periventricular edema. (B) Sagittal contrast-enhanced T1-weighted image shows peripherally predominant enhancement of the tumor. Partially restricted diffusion (not shown) also was observed.

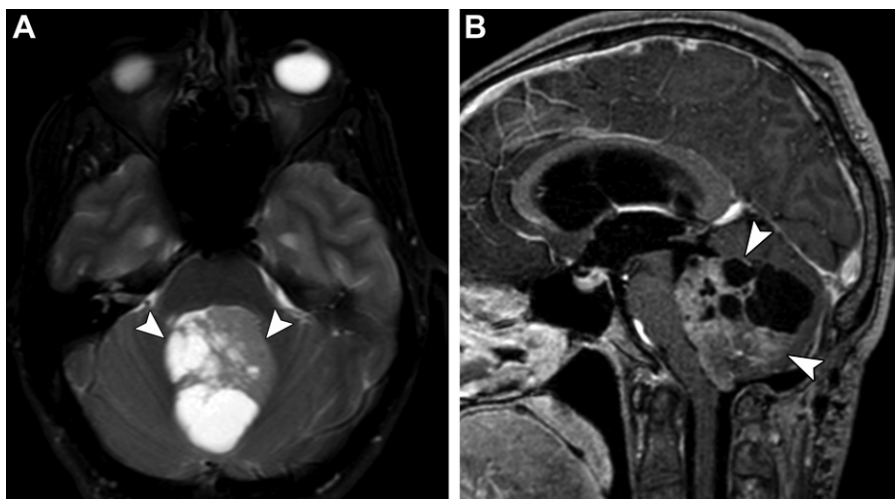


**Figure 20.** Posterior fossa ependymoma, group PFB, in a 36-year-old man who presented with a headache and gait disturbances. MR images show a lobulated intraventricular tumor (arrowheads) in the fourth ventricle, with secondary hydrocephalus. (A) Axial T2-weighted fat-suppressed image shows the tumor to have heterogeneous hyperintensity, with multiple cystic components. (B) Sagittal contrast-enhanced T1-weighted image shows heterogeneous enhancement of the solid components of the tumor. Restricted diffusion also was seen (not shown).

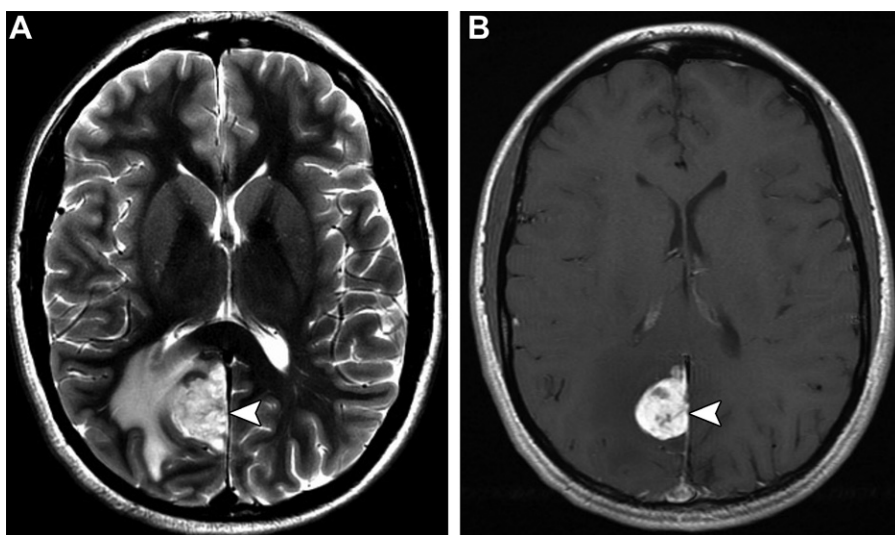


**Figure 21.** Intracranial mesenchymal tumor, *FET-CREB fusion-positive*, in a 29-year-old woman with a sudden-onset severe headache, abnormal mental status, and anemia. (A) Axial T2-weighted MR image shows a solid-cystic mass (arrowhead) attached to the falx cerebri, with surrounding parenchymal edema. (B) Axial contrast-enhanced T1-weighted MR image shows strong enhancement of the solid portion of the tumor (arrowhead).

provisional tumors currently await comprehensive published characterization but will likely become fully recognized tumor types in a future classification iteration.

### Conclusion

We have reviewed the major revisions in WHO CNS5 and summarized the molecular, clinical, and imaging features of the newly recognized CNS tumor types and subtypes. The WHO CNS5 classification system has become the foundation for daily practice, replacing the fourth edition of the WHO CNS classification system. However, as emphasized by Louis et al (2), these classifications should be regarded as being in the provisional stage of the evolution of CNS tumor classifications. Future studies, reviews, task forces, and integrated assessments need to be used to evaluate these tumor delineations and classifications more thoroughly. Hence, our review is intended to guide future research and inform medical guidelines.

**Disclosures of conflicts of interest.**—E.L. Educational subsidy for meeting attendance from Michigan Medicine, University of Michigan.

### References

1. Louis DN, Perry A, Reifenberger G, et al. The 2016 World Health Organization Classification of Tumors of the Central Nervous System: a summary. *Acta Neuropathol (Berl)* 2016;131(6):803–820.
2. Louis DN, Perry A, Wesseling P, et al. The 2021 WHO Classification of Tumors of the Central Nervous System: a summary. *Neuro Oncol* 2021;23(8):1231–1251.
3. Louis DN, Wesseling P, Paulus W, et al. cIMPACT-NOW update 1: not otherwise specified (NOS) and not elsewhere classified (NEC). *Acta Neuropathol (Berl)* 2018;135(3):481–484.
4. Louis DN, Giannini C, Capper D, et al. cIMPACT-NOW update 2: diagnostic clarifications for diffuse midline glioma, H3 K27M-mutant and diffuse astrocytoma/anaplastic astrocytoma, IDH-mutant. *Acta Neuropathol (Berl)* 2018;135(4):639–642.
5. Brat DJ, Aldape K, Colman H, et al. cIMPACT-NOW update 3: recommended diagnostic criteria for “diffuse astrocytic glioma, IDH-wildtype, with molecular features of glioblastoma, WHO grade IV.” *Acta Neuropathol (Berl)* 2018;136(5):805–810.
6. Ellison DW, Hawkins C, Jones DTW, et al. cIMPACT-NOW update 4: diffuse gliomas characterized by MYB,

- MYBL1, or FGFR1 alterations or BRAF<sup>V600E</sup> mutation. *Acta Neuropathol (Berl)* 2019;137(4):683–687.
7. Brat DJ, Aldape K, Colman H, et al. cIMPACT-NOW update 5: recommended grading criteria and terminologies for IDH-mutant astrocytomas. *Acta Neuropathol (Berl)* 2020;139(3):603–608.
  8. Louis DN, Wesseling P, Aldape K, et al. cIMPACT-NOW update 6: new entity and diagnostic principle recommendations of the cIMPACT-Utrecht meeting on future CNS tumor classification and grading. *Brain Pathol* 2020;30(4):844–856.
  9. Ellison DW, Aldape KD, Capper D, et al. cIMPACT-NOW update 7: advancing the molecular classification of ependymal tumors. *Brain Pathol* 2020;30(5):863–866.
  10. Zulch KJ. Histological typing of tumours of the central nervous system. In: International histological classification of tumours No 21. Geneva, Switzerland: World Health Organization, 1979; 19–24.
  11. Kleihues P, Burger PC, Scheithauer BW. Histological typing of tumours of the central nervous system. Heidelberg, Germany: Springer-Verlag Berlin, 1993.
  12. Kleihues P, Burger PC, Scheithauer BW. The new WHO classification of brain tumours. *Brain Pathol* 1993;3(3):255–268.
  13. Kleihues P, Cavenee WK. Pathology and genetics of tumours of the Nervous System. Lyon, France: IARC Press, 2000.
  14. Louis DN, Ohgaki H, Wiestler OD, et al. The 2007 WHO classification of tumours of the central nervous system. *Acta Neuropathol (Berl)* 2007;114(2):97–109.
  15. Louis DN, Ellison DW, Brat DJ, et al. cIMPACT-NOW: a practical summary of diagnostic points from round 1 updates. *Brain Pathol* 2019;29(4):469–472.
  16. Sahm F, Reuss D, Koelsche C, et al. Farewell to oligoastrocytoma: in situ molecular genetics favor classification as either oligodendrogloma or astrocytoma. *Acta Neuropathol (Berl)* 2014;128(4):551–559.
  17. Kros JM, Gorlia T, Kouwenhoven MC, et al. Panel review of anaplastic oligodendrogloma from European Organization for Research and Treatment of Cancer Trial 26951: assessment of consensus in diagnosis, influence of 1p/19q loss, and correlations with outcome. *J Neuropathol Exp Neurol* 2007;66(6):545–551.
  18. Xia L, Wu B, Fu Z, et al. Prognostic role of IDH mutations in gliomas: a meta-analysis of 55 observational studies. *Oncotarget* 2015;6(19):17354–17365.
  19. Picart T, Barriault M, Poncet D, et al. Characteristics of diffuse hemispheric gliomas, H3 G34-mutant in adults. *Neurooncol Adv* 2021;3(1):vdab061.
  20. Lowe BR, Maxham LA, Hamey JJ, Wilkins MR, Partridge JF. Histone H3 mutations: an updated view of their role in chromatin deregulation and cancer. *Cancers (Basel)* 2019;11(5):660.
  21. Sievers P, Sill M, Schrimpf D, et al. A subset of pediatric-type thalamic gliomas share a distinct DNA methylation profile, H3K27me3 loss and frequent alteration of EGFR. *Neuro Oncol* 2021;23(1):34–43.
  22. Johnson DR, Guerin JB, Giannini C, Morris JM, Eckel LJ, Kaufmann TJ. 2016 updates to the WHO Brain Tumor Classification system: what the radiologist needs to know. *RadioGraphics* 2017;37(7):2164–2180.
  23. Qaddoumi I, Orisme W, Wen J, et al. Genetic alterations in uncommon low-grade neuroepithelial tumors: BRAF, FGFR1, and MYB mutations occur at high frequency and align with morphology. *Acta Neuropathol (Berl)* 2016;131(6):833–845.
  24. Santarpia L, Lippman SM, El-Naggar AK. Targeting the MAPK-RAS-RAF signaling pathway in cancer therapy. *Expert Opin Ther Targets* 2012;16(1):103–119.
  25. Wefers AK, Stichel D, Schrimpf D, et al. Isomorphic diffuse glioma is a morphologically and molecularly distinct tumour entity with recurrent gene fusions of MYBL1 or MYB and a benign disease course. *Acta Neuropathol (Berl)* 2020;139(1):193–209.
  26. Johnson DR, Giannini C, Jenkins RB, Kim DK, Kaufmann TJ. Plenty of calcification: imaging characterization of polymorphous low-grade neuroepithelial tumor of the young. *Neuroradiology* 2019;61(11):1327–1332.
  27. Huse JT, Snuderl M, Jones DTW, et al. Polymorphous low-grade neuroepithelial tumor of the young (PLNTY): an epileptogenic neoplasm with oligodendrogloma-like components, aberrant CD34 expression, and genetic alterations involving the MAP kinase pathway. *Acta Neuropathol (Berl)* 2017;133(3):417–429.
  28. Kurokawa M, Kurokawa R, Capizzano AA, et al. Neuroradiological features of the polymorphous low-grade neuroepithelial tumor of the young: five new cases with a systematic review of the literature. *Neuroradiology* 2022. 10.1007/s00234-021-02879-5. Published online January 10, 2022.
  29. Kurokawa R, Baba A, Kurokawa M, et al. Neuroimaging features of diffuse hemispheric glioma, H3 G34-mutant: a case series and systematic review. *J Neuroimaging* 2022;32(1):17–27.
  30. Mackay A, Burford A, Carvalho D, et al. Integrated molecular meta-analysis of 1,000 pediatric high-grade and diffuse intrinsic pontine glioma. *Cancer Cell* 2017;32(4):520–537.e5.
  31. Korshunov A, Capper D, Reuss D, et al. Histologically distinct neuroepithelial tumors with histone 3 G34 mutation are molecularly similar and comprise a single nosologic entity. *Acta Neuropathol (Berl)* 2016;131(1):137–146.
  32. Gonçalves FG, Viaene AN, Vossough A. Advanced magnetic resonance imaging in pediatric glioblastomas. *Front Neurol* 2021;12:73323.
  33. Guerreiro Stucklin AS, Ryall S, Fukuoka K, et al. Alterations in ALK/ROS1/NTRK/MET drive a group of infantile hemispheric gliomas. *Nat Commun* 2019;10(1):4343.
  34. Reinhardt A, Stichel D, Schrimpf D, et al. Anaplastic astrocytoma with piloid features, a novel molecular class of IDH wildtype glioma with recurrent MAPK pathway, CDKN2A/B and ATRX alterations. *Acta Neuropathol (Berl)* 2018;136(2):273–291.
  35. Bender K, Perez E, Chirica M, et al. High-grade astrocytoma with piloid features (HGAP): the Charité experience with a new central nervous system tumor entity. *J Neurooncol* 2021;153(1):109–120.
  36. Lucas CG, Villanueva-Meyer JE, Whipple N, et al. Myxoid glioneuronal tumor, PDGFRA p.K385-mutant: clinical, radiologic, and histopathologic features. *Brain Pathol* 2020;30(3):479–494.
  37. Solomon DA, Korshunov A, Sill M, et al. Myxoid glioneuronal tumor of the septum pellucidum and lateral ventricle is defined by a recurrent PDGFRA p.K385 mutation and DNT-like methylation profile. *Acta Neuropathol (Berl)* 2018;136(2):339–343.
  38. Narvaez EO, Inada BSY, de Almeida PRSF, et al. Myxoid glioneuronal tumour: report of three cases of a new tumour in a typical location and review of literature. *BJR Case Rep* 2021;7(4):20200139.
  39. Pekmezci M, Stevers M, Phillips JJ, et al. Multinodular and vacuolating neuronal tumor of the cerebrum is a clonal neoplasm defined by genetic alterations that activate the MAP kinase signaling pathway. *Acta Neuropathol (Berl)* 2018;135(3):485–488.
  40. Buffa GB, Chaves H, Serra MM, Stefanoff NI, Gagliardo AS, Yáñez P. Multinodular and vacuolating neuronal tumor of the cerebrum (MVNT): a case series and review of the literature. *J Neuroradiol* 2020;47(3):216–220.
  41. Nunes RH, Hsu CC, da Rocha AJ, et al. Multinodular and vacuolating neuronal tumor of the cerebrum: a new “leave me alone” lesion with a characteristic imaging pattern. *AJR Am J Neuroradiol* 2017;38(10):1899–1904.
  42. Lecler A, Bailleux J, Carsin B, et al. Multinodular and vacuolating posterior fossa lesions of unknown significance. *AJR Am J Neuroradiol* 2019;40(10):1689–1694.
  43. Agarwal A, Lakshmanan R, Devagnamam I, Bynevelt M. Multinodular and vacuolating neuronal tumor of the cerebrum: does the name require review? *AJR Am J Neuroradiol* 2019;40(12):E69–E70.
  44. Morassi M, Bagatto D. Infratentorial multinodular and vacuolating neuronal tumor or multinodular and vacuolating posterior fossa lesions of unknown significance? clinico-radiologic findings from 2 cases. *World Neurosurg* 2020;136:58–61.
  45. Furuta T, Moritsubo M, Muta H, et al. Central nervous system neuroblastic tumor with FOXR2 activation presenting

- both neuronal and glial differentiation: a case report. *Brain Tumor Pathol* 2020;37(3):100–104.
46. Holsten T, Lubieniecki F, Spohn M, et al. Detailed clinical and histopathological description of 8 cases of molecularly defined CNS neuroblastomas. *J Neuropathol Exp Neurol* 2021;80(1):52–59.
  47. Yoshida Y, Nobusawa S, Nakata S, et al. CNS high-grade neuroepithelial tumor with BCOR internal tandem duplication: a comparison with its counterparts in the kidney and soft tissue. *Brain Pathol* 2018;28(5):710–720.
  48. Cardoen L, Tauziède-Espriat A, Dangouloff-Ros V, et al. Imaging features with histopathologic correlation of CNS high-grade neuroepithelial tumors with a BCOR internal tandem duplication. *AJNR Am J Neuroradiol* 2022;43(1):151–156.
  49. Thomas C, Wefers A, Bens S, et al. Desmoplastic myxoid tumor, SMARCB1-mutant: clinical, histopathological and molecular characterization of a pineal region tumor encountered in adolescents and adults. *Acta Neuropathol (Berl)* 2020;139(2):277–286.
  50. Wang YE, Chen JJ, Wang W, Zhang AL, Zhou W, Wu HB. A case of desmoplastic myxoid tumor, SMARCB1 mutant, in the pineal region. *Neuropathology* 2021;41(1):37–41.
  51. Matsumura N, Goda N, Yashige K, et al. Desmoplastic myxoid tumor, SMARCB1-mutant: a new variant of SMARCB1-deficient tumor of the central nervous system preferentially arising in the pineal region. *Virchows Arch* 2021;479(4):835–839.
  52. Pratt D, Kumar-Sinha C, Cieślik M, et al. A novel ATXN1-DUX4 fusion expands the spectrum of ‘CIC-rearranged sarcoma’ of the CNS to include non-CIC alterations. *Acta Neuropathol (Berl)* 2021;141(4):619–622.
  53. Yamada S, Muto J, De Leon JCA, et al. Primary spinal intramedullary Ewing-like sarcoma harboring CIC-DUX4 translocation: a similar cytological appearance as its soft tissue counterpart but no lobulation in association with desmoplastic stroma. *Brain Tumor Pathol* 2020;37(3):111–117.
  54. Bernstein E, Caudy AA, Hammond SM, Hannon GJ. Role for a bidentate ribonuclease in the initiation step of RNA interference. *Nature* 2001;409(6818):363–366.
  55. Kamihara J, Paulson V, Breen MA, et al. DICER1-associated central nervous system sarcoma in children: comprehensive clinicopathologic and genetic analysis of a newly described rare tumor. *Mod Pathol* 2020;33(10):1910–1921.
  56. Diaz Coronado RY, Mynarek M, Koelsche C, et al. Primary central nervous system sarcoma with DICER1 mutation—treatment results of a novel molecular entity in pediatric Peruvian patients. *Cancer* 2022;128(4):697–707.
  57. de Kock L, Sabbaghian N, Plourde F, et al. Pituitary blastoma: a pathognomonic feature of germ-line DICER1 mutations. *Acta Neuropathol (Berl)* 2014;128(1):111–122.
  58. Liu APY, Kelsey MM, Sabbaghian N, et al. Clinical outcomes and complications of pituitary blastoma. *J Clin Endocrinol Metab* 2021;106(2):351–363.
  59. Scheithauer BW, Kovacs K, Horvath E, et al. Pituitary blastoma. *Acta Neuropathol (Berl)* 2008;116(6):657–666.
  60. Chhuon Y, Weon YC, Park G, Kim M, Park JB, Park SK. Pituitary blastoma in a 19-year-old Woman: a case report and review of literature. *World Neurosurg* 2020;139:310–313.
  61. Andreuolo F, Varlet P, Tauziède-Espriat A, et al. Childhood supratentorial ependymomas with YAP1-MAML1 fusion: an entity with characteristic clinical, radiological, cytogenetic and histopathological features. *Brain Pathol* 2019;29(2):205–216.
  62. Pajtler KW, Witt H, Sill M, et al. Molecular classification of ependymal tumors across all CNS compartments, histopathological grades, and age groups. *Cancer Cell* 2015;27(5):728–743.
  63. Yonezawa U, Karlowee V, Amatya VJ, et al. Radiology profile as a potential instrument to differentiate between posterior fossa ependymoma (PF-EPN) group A and B. *World Neurosurg* 2020;140:e320–e327.
  64. Liu R, Shi P, Wang Z, Yuan C, Cui H. Molecular mechanisms of MYCN dysregulation in cancers. *Front Oncol* 2021;10:625332.
  65. Raffeld M, Abdullaev Z, Pack SD, et al. High level MYCN amplification and distinct methylation signature define an aggressive subtype of spinal cord ependymoma. *Acta Neuropathol Commun* 2020;8(1):101.
  66. Swanson AA, Raghu Nath A, Jenkins RB, et al. Spinal cord ependymomas with MYCN amplification show aggressive clinical behavior. *J Neuropathol Exp Neurol* 2019;78(9):791–797.